

## Structure-Based Design of Novel, Urea-Containing FKBP12 Inhibitors

Peter S. Dragovich,\* John E. Barker, Judy French, Michael Imbacuan, Vincent J. Kalish, Charles R. Kissinger, Daniel R. Knighton, Cristina T. Lewis, Ellen W. Moomaw, Hans E. Parge, Laura A. K. Pelletier, Thomas J. Prins, Richard E. Showalter, John H. Tatlock, Kathleen D. Tucker, and J. Ernest Villafranca

Agouron Pharmaceuticals, Inc., 3565 General Atomics Court, San Diego, California 92121

Received October 30, 1995<sup>®</sup>

The structure-based design and subsequent chemical synthesis of novel, urea-containing FKBP12 inhibitors are described. These compounds are shown to disrupt the cis–trans peptidylprolyl isomerase activity of FKBP12 with inhibition constants ( $K_{i,app}$ ) approaching 0.10  $\mu$ M. Analyses of several X-ray crystal structures of FKBP12–urea complexes demonstrate that the urea-containing inhibitors associate with FKBP12 in a manner that is similar to, but significantly different from, that observed for the natural product FK506.

### Introduction

FK506 (tacrolimus, Figure 1) is a potent immunosuppressive natural product whose mechanism of action has recently been elucidated at the cellular level.<sup>1,2</sup> FK506 strongly associates with the immunophilin FKBP12 (FK506-binding protein), a member of a ubiquitous family of proteins which catalyze the cis–trans isomerization of peptidyl proline amide bonds.<sup>3,4</sup> FK506 potently inhibits FKBP12 isomerase activity, presumably by binding as a transition state analog, and it was initially speculated that such isomerase inhibition was responsible for the immunosuppressive properties which the molecule displays.<sup>5</sup> This theory was supported by the earlier finding that the structurally unrelated immunosuppressant cyclosporin A (CsA) inhibits the function of a different cellular target, cyclophilin (cyclosporin-binding protein, CyP), which also possesses isomerase activity.<sup>6,7</sup> However, rapamycin, another highly immunosuppressive natural product, also potently inhibits FKBP12 isomerase activity but antagonizes FK506-related immunosuppressive effects.<sup>8,9</sup> Additional experiments have established that the complex formed by FK506 and FKBP12 inhibits the function of a second cellular target, the calcium-dependent, calmodulin-activated protein phosphatase calcineurin (CN, PP2B).<sup>10,11</sup> This inhibition, in turn, is believed to prevent nuclear translocation of the NF-AT (nuclear factor of activated T-cells) cytosolic component thereby blocking  $Ca^{2+}$ -dependent IL-2 gene transcription necessary for T-cell activation.<sup>12</sup>

It has been implied from the above experimental data that FK506 can be divided into two distinct regions: one which associates with FKBP12 and one which contacts calcineurin upon formation of the FKBP12–FK506 complex.<sup>13</sup> The former region, the binding domain, contains the pipercolinic acid  $\alpha$ -ketoamide functional group and extends from the pyranose fragment on one side of the molecule to the cyclohexyl group on the other. The latter domain, the effector region, includes portions of the remainder of the molecule. Such assignments are supported by NMR solution structures<sup>14</sup> and X-ray crystal structures<sup>15</sup> of FK506 complexed with FKBP12 and were recently confirmed by the determination of the X-ray crystal structures of the calcineurin–FKBP12–FK506 ternary complex.<sup>16</sup> An important conclusion of

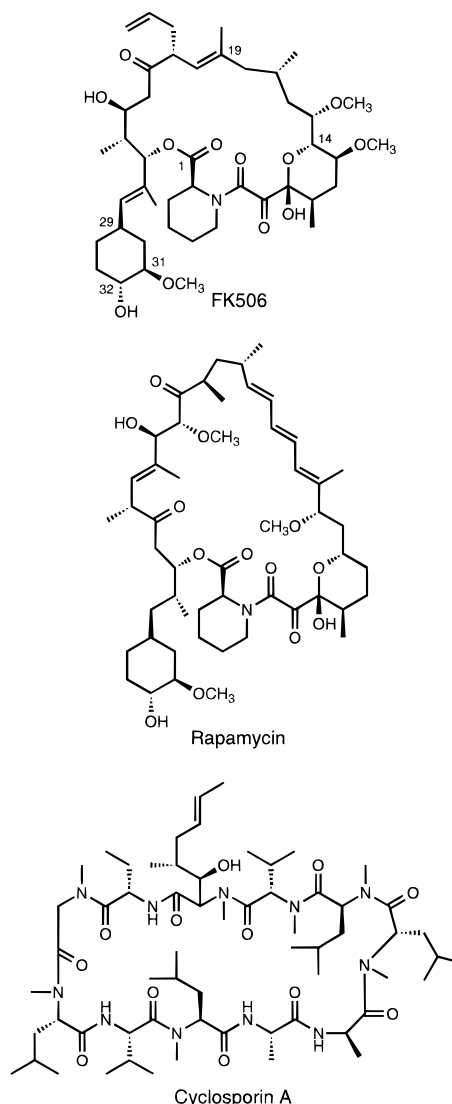


**Figure 1.** Natural product immunosuppressants.

the dual-domain hypothesis is that only molecules which incorporate both functional domains would be expected to exhibit immunosuppressive effects similar to those induced by FK506. Indeed, the synthetic molecule 506BD, which contains the FKBP12-binding domain of FK506 but lacks an appropriate effector region, potently inhibits FKBP12 isomerase activity but displays no immunosuppressive properties.<sup>13,17</sup> In addition, selected

<sup>®</sup> Abstract published in *Advance ACS Abstracts*, March 1, 1996.

alterations to either the effector region of FK506 or certain FKBP12 residues which surround the FK506-binding pocket can diminish the immunosuppressive properties of the corresponding FKBP12–FK506 complexes (presumably by disrupting their association with calcineurin) without significantly affecting FKBP12–FK506 interactions.<sup>18,19</sup> Such results, coupled with the X-ray analysis of the calcineurin–FKBP12–FK506 ternary complex,<sup>16</sup> indicate that elements of both FK506 and FKBP12 contribute to a composite surface which is recognized by calcineurin and underscore the need for FK506-like immunosuppressants to associate with FKBP12 in a manner that does not preclude the formation of such a surface.

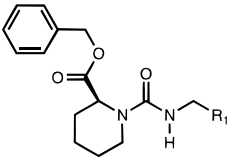
### Inhibitor Design and Structure–Activity Studies

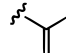
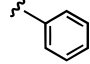
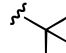
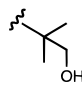
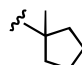
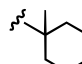
As part of a program to develop novel immunosuppressants that function in a manner similar to that of FK506, we sought to design simple FKBP12-binding moieties to which potential effector regions could be attached. The apparent inhibition constant of FKBP12 isomerase activity ( $K_{i,app}$ ) exhibited by a molecule binding at the FKBP12 active site is known to correlate well with measured dissociation constants ( $K_d$ ).<sup>20a,b</sup> This inhibition constant can be accurately determined by known assay techniques and was therefore chosen for use in this study as an indicator of FKBP12–ligand association strength (full details of the biochemical assay methods are presented in the Experimental Section).

Small synthetic molecules which incorporate a (S)-pipecolyl-derived  $\alpha$ -ketoamide moiety are known to be potent inhibitors of FKBP12 isomerase activity ( $K_{i,app} = 1$ –100 nM).<sup>20</sup> However, in an effort to obtain immunosuppressive compounds with pharmacological profiles that differed from FK506, the development of FKBP12 inhibitors which did not contain the  $\alpha$ -ketoamide functional group was considered. Molecules belonging to this category are typically not potent FKBP12 inhibitors,<sup>21</sup> although several groups have reported sub-micromolar FKBP12 isomerase inhibition by pipecolyl-derived sulfonamides.<sup>22</sup> In addition, it was reasoned that an ideal binding moiety would depart the FKBP12 active site in a manner similar to that observed for FK506 in order to facilitate the future design of effector regions which spatially resemble the natural product.

The above considerations led to the general design of an inhibitor in which the  $\alpha$ -ketoamide functional group typically found in potent FKBP12-binding molecules was replaced by a urea moiety (Table 1). Such a molecule would forfeit the beneficial interactions made by the  $\alpha$ -ketoamide ketone carbonyl with the  $\epsilon$ -hydrogens of three aromatic FKBP12 residues on the floor of the binding cavity (Tyr-26, Phe-36, and Phe-99) but was anticipated to form a hydrogen bond between the urea NH and the carboxylate of Asp-37 analogous to that made by the hemiketal hydroxyl group of FK506.<sup>14,15</sup> Analysis of computer-generated models suggested that, due to the planar geometry of the urea functional group, inclusion of a methylene unit adjacent to the urea NH would allow appended moieties ( $R_1$ ) to better contact the FKBP12 residues which interact with the FK506 pyranose ring (Phe-36, Ile-90, Ile-91, and His-87). The development of two series of urea-containing compounds

Table 1

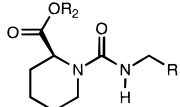


Compd No.	$R_1$	$K_{i, app}$ ( $\mu$ M)
1		7.2
2		6.5
3		0.79
4		8.4
5		0.57
6		0.55

which function as inhibitors of FKBP12 isomerase activity is described below.

Initially, the identification of an appropriate FK506 pyranose mimetic for incorporation into an acyclic urea derived from (S)-pipecolinic acid benzyl ester was undertaken. Since previous studies of  $\alpha$ -ketoamide-containing FKBP12 inhibitors had demonstrated that large hydrophobic groups could function as effective pyranose mimics, the inclusion of similar moieties in the urea series seemed appropriate.<sup>20</sup> Accordingly, a number of ureas were prepared by combining (S)-pipecolinic acid benzyl ester with various primary amines which incorporated hydrophobic moieties of differing sizes (Table 1). Ureas containing small (**1**) or flat (**2**) hydrophobic pyranose replacement groups displayed moderate FKBP12 inhibition levels in the low micromolar range. Incorporation of the larger *tert*-butyl moiety into the urea design substantially increased the FKBP12 affinity of the resulting inhibitor (compare **2** and **3**). Inclusion of an unprotected hydroxyl group in this portion of the inhibitor (**4**) was detrimental to FKBP12 affinity, presumably due to poor interactions with the hydrophobic FKBP12 residues which contact the pyranose mimics. Crystallographic analysis of the FKBP12–**3** complex indicated that additional protein–ligand hydrophobic interactions could be realized by incorporating a portion of the *tert*-butyl moiety into a hydrocarbon ring. Accordingly, compounds **5** and **6** were prepared with such a modification, and both inhibited FKBP12 more potently than compound **3**. The preparation of compounds **5** and **6** concluded the development of pyranose mimics for use with the acyclic urea series. However, since molecules which contained the cyclic pyranose mimics proved more difficult to crystallize with FKBP12 than their *tert*-butyl counterparts, the latter fragment was utilized in many subsequent inhibitor designs.

Table 2



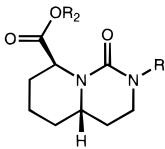
Compd No.	R <sub>1</sub>	R <sub>2</sub>	K <sub>i,app</sub> (μM)
7			0.35
8	<i>a</i>		0.39
9	<i>a</i>		0.37
10	<i>a</i>		0.22
11	<i>a</i>		0.15
12			0.20
13	<i>a</i>		0.12

<sup>a</sup> Same as above.

Having identified several suitable pyranose replacements for use in the development of the urea-containing inhibitors, variation of the ester functionality was then examined with the dual purpose of providing increased FKBP12 affinity and a departure point for the subsequent attachment of appropriate effector regions (Table 2). Incorporation of simplified versions of the FK506 cyclohexyl moiety (C<sub>29</sub>–C<sub>34</sub>) into the inhibitor design increased the FKBP12 affinity of the resulting compounds 2–5-fold as compared to their benzyl ester counterparts. Initially, it was believed that the increased FKBP12 affinity displayed by all of these compounds was derived from additional hydrophobic interactions between the larger ester fragments and the region of FKBP12 which contacts the FK506 cyclohexyl moiety. However, crystallographic analysis of the FKBP12–**8** complex revealed this assumption to be incorrect and also suggested that the corresponding 3-(3-methoxyphenyl)propyl ester should display similar FKBP12 affinity. This prediction was verified experimentally with the preparation and evaluation of compound **9** (Table 2). Replacement of the *tert*-butyl pyranose mimetics of the most active molecules with the larger cyclohexyl moiety resulted in slightly more potent FKBP12 inhibitors relative to the original compounds (compare **10** with **12** and **11** with **13**). These ureas rank among the most potent non- $\alpha$ -ketoamide-containing FKBP12 inhibitors reported to date and should function as suitable FKBP12-binding moieties for the attachment of appropriate effector regions.<sup>23</sup>

In addition to the acyclic ureas described above, the development of a series of cyclic ureas as FKBP12

Table 3



compd no. <sup>a</sup>	R <sub>1</sub>	R <sub>2</sub>	K <sub>i,app</sub> (μM)
<b>14</b>	CH <sub>2</sub> Ph	CH <sub>3</sub>	67
<b>15</b>	<i>b</i>	CH <sub>2</sub> Ph	14
<b>16</b>	CH <sub>2</sub> CH <sub>2</sub> CH <sub>3</sub>	CH <sub>3</sub>	83
<b>17</b>	<i>b</i>	CH <sub>2</sub> Ph	24

<sup>a</sup> Prepared in racemic form. <sup>b</sup> Same as above.

inhibitors was also undertaken (Table 3). Although such compounds would forfeit the presumed hydrogen bonding interactions of the acyclic ureas with Asp-37 of the protein, their cyclic nature would prevent *cis*–*trans* isomer equilibration and thus potentially increase FKBP12 affinity by rigidifying the inhibitor in a beneficial conformation. Computational analysis utilizing the FKBP12–FK506 crystal structure<sup>15</sup> suggested that the proposed bicyclic framework could be accommodated in the FKBP12 active site with small movements of Asp-37 and Tyr-82 outward from the center of the binding pocket. Since the binding geometry of the acyclic and cyclic ureas was expected to be similar, it was anticipated that structure–activity information gained from development of the former inhibitor series could be utilized for optimization of the latter. In the event, several racemic cyclic ureas were prepared and displayed mid to low micromolar levels of FKBP12 inhibition (Table 3). However, crystallographic analysis of the FKBP12–**17** complex revealed that the binding geometry of the cyclic urea was significantly different from that observed for the related acyclic molecules described above and suggested that independent structure–activity studies would be required for optimization of the new compounds. Therefore, subsequent synthetic efforts were focused on the development of the more easily prepared acyclic urea series.

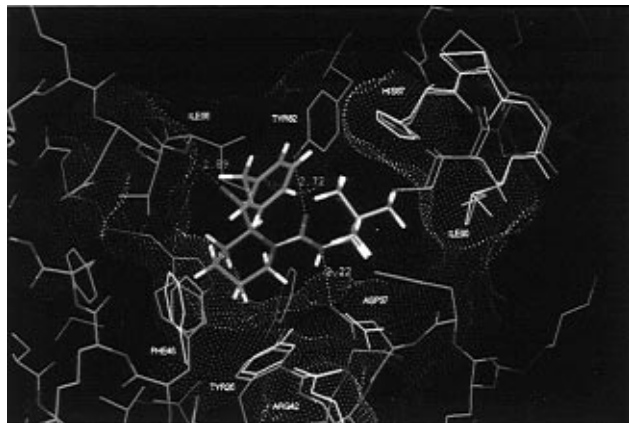
### X-ray Structure Analyses

The iterative analysis of protein–ligand interactions by X-ray crystallography is an essential element of a structure-based inhibitor design program.<sup>24</sup> Accordingly, several crystal structures of FKBP12–inhibitor complexes were obtained during the development of the urea-containing compounds described above. These structures established the binding geometries that the urea inhibitors adopted when complexed with FKBP12, suggested improvements for ligand design, allowed comparison of FKBP12–urea interactions with those reported for related  $\alpha$ -ketoamide inhibitors (including FK506), and identified departure points from the FKBP12-binding pocket for subsequent effector region attachment. An overview of the general characteristics of the FKBP12–urea crystal structures obtained is presented below followed by discussion of specific details that were observed in individual FKBP12–inhibitor complexes.

The overall FKBP12 structure observed for all new FKBP12–inhibitor complexes was not significantly dif-

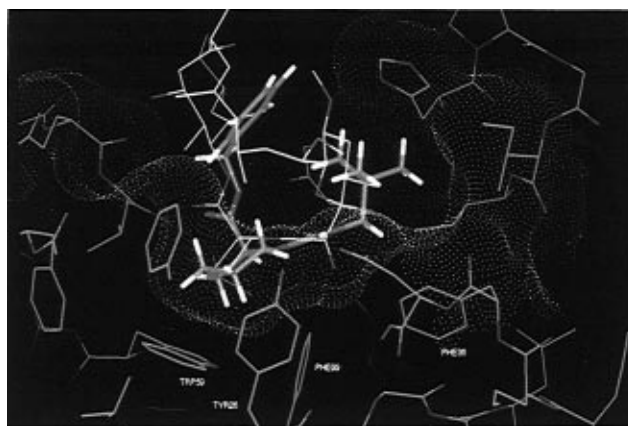
**Table 4.** Root-Mean-Square Differences between Atom Positions of FKBP12–FK506 and FKBP12–Ligand Complexes

compd no.	$\alpha$ -carbons	backbone atoms
<b>3</b>	0.39	0.40
<b>4</b>	0.38	0.38
<b>7</b>	0.40	0.40
<b>8</b>	0.50	0.48
<b>9</b>	0.53	0.53
<b>17</b>	0.38	0.39

**Figure 2.** Crystal structure of the FKBP12–3 complex. Hydrogen bonds are indicated as white dashed lines. A portion of the water-accessible surface of the protein is shown as pink dots. Selected side chains of FKBP12 residues from the FKBP12–FK506 crystal structure are superimposed and shown in yellow.

ferent from that found in the uncomplexed protein or the FKBP12–FK506 or FKBP12–rapamycin crystal structures.<sup>14,15,25</sup> Comparison of the FKBP12–inhibitor complexes with that of FKBP12–FK506 revealed small root-mean-square (rms) deviations between  $\alpha$ -carbon atom positions as well as backbone atom locations (Table 4). Similar gross protein structure was reported for the complexes formed between FKBP12 and several non-macrocyclic  $\alpha$ -ketoamide inhibitors.<sup>15d,20b</sup>

The acyclic urea inhibitors, typified by compound **3**, bound to FKBP12 in a manner that was similar to, but significantly different from, that observed for related  $\alpha$ -ketoamide-containing inhibitors such as FK506. The pipercolyl ring of each compound was positioned above the indole side chain of Trp-59, with hydrogen bonds observed between the pipercolyl ester carbonyl and Ile-56-NH and between the urea carbonyl and Tyr-82-OH (Figures 2 and 3). Comparable inhibitor locations and hydrogen-bonding interactions have been observed in crystal structures of related  $\alpha$ -ketoamides complexed with FKBP12.<sup>20b,i</sup> As anticipated, an additional (albeit long) hydrogen bond was observed between the urea NH and the carboxylate of Asp-37, accompanied by movement of the Asp-37 side chain toward the inhibitor (typically 0.87 Å relative to its position observed in the FKBP12–FK506 complex). Other FKBP12 residues which form hydrogen bonds with Asp-37 (Arg-42 and Tyr-26) also moved slightly from their observed locations in the FKBP12–FK506 crystal structure. In addition, movement (~1.1 Å) of the Phe-46 aromatic side chain toward the inhibitor (relative to its position in the FKBP12–FK506 structure) was also observed in many FKBP12–urea complexes (Figure 2). This movement probably results from the absence of inhibitor functionality which mimics the C<sub>19</sub> methyl group of FK506. This

**Figure 3.** Crystal structure of the FKBP12–3 complex (alternate view). A portion of the water-accessible surface of the protein is shown as pink dots. FK506 (hydrogen atoms omitted) from the FKBP12–FK506 crystal structure is superimposed and shown in yellow.

methyl group contacts the side chain of Phe-46 in the FKBP12–FK506 complex and most likely influences its crystallographically observed position. Importantly, the locations at which the acyclic urea inhibitors exited the FKBP12-binding cavity were spatially similar to those observed for FK506 in the FKBP12–FK506 complex, presumably simplifying the task of subsequent effector region design.

One of the most surprising aspects of the FKBP12–inhibitor crystal structures was the binding geometry adopted by the pipercolyl fragment of the urea ligands (Figure 3). This geometry was significantly different from that observed for related pipercolyl-derived  $\alpha$ -ketoamides (such as FK506) and resulted in a departure of the urea functional group from the plane defined by the FK506 amide moiety. Due to the planar nature of the urea, the locations of attached pyranose mimetics were also altered slightly from the position of the FK506 pyranose moiety. In addition, the three aromatic FKBP12 residues on the floor of the active site whose  $\epsilon$ -hydrogens interact with the FK506 ketone carbonyl moiety (Tyr-26, Phe-36, and Phe-99) did not move appreciably from their locations in the FKBP12–FK506 complex. Thus, a significant gap between protein and ligand was observed directly below the urea NH in all the FKBP12–inhibitor complexes examined (Figure 3). The presence of this, presumably unfavorable, gap in the FKBP12–urea complexes may be primarily responsible for the somewhat weaker FKBP12 affinity exhibited by a typical acyclic urea inhibitor relative to similar  $\alpha$ -ketoamide-containing compounds.<sup>20</sup>

In spite of the altered binding geometry described above, good hydrophobic interactions were observed between the *tert*-butyl group of compound **3** and the FKBP12 residues which interact with the FK506 pyranose moiety (Phe-36, Ile-90, Ile-91, and His-87; Figures 2 and 3). Importantly, the positions of these residues in the FKBP12–**3** complex were virtually unchanged from their locations in the FKBP12–FK506 crystal structure (Figure 2). Since crystallographic analysis of the calcineurin–FKBP12–FK506 ternary complex has established that this region of FKBP12 forms part of the composite surface which interacts with calcineurin, the ability of the urea inhibitors to associate with FKBP12 without perturbing these residues was note-

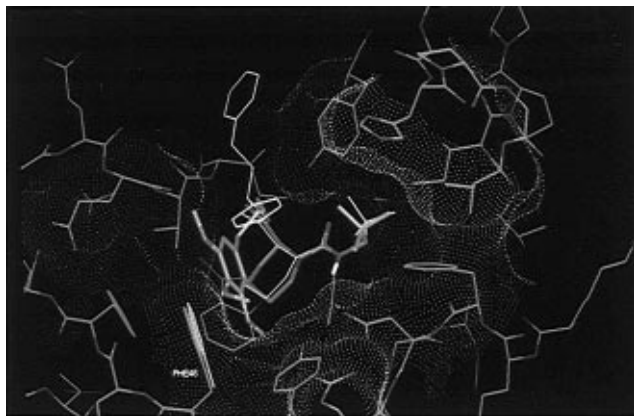


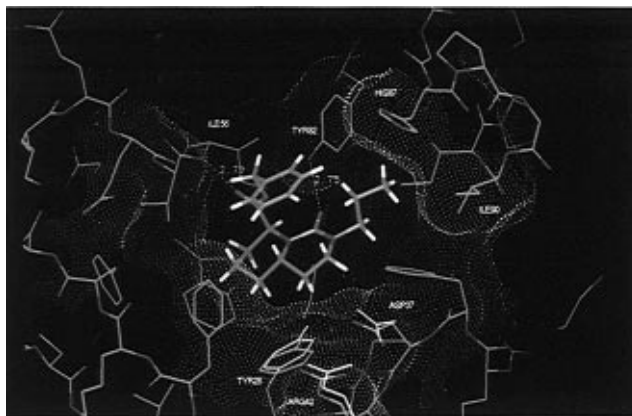
**Figure 4.** Crystal structure of the FKBP12-8 complex. The ligand 7 is superimposed and shown in gray. Hydrogen atoms have been omitted from both compounds 7 and 8 for clarity. A portion of the water-accessible FKBP12 surface is shown as pink dots. The side chain of Phe-46 from the FKBP12-FK506 crystal structure is superimposed and shown in yellow.

worthy.<sup>16,26</sup> In addition, the benzyl ester fragment of **3** made favorable inter- and intramolecular hydrophobic contacts with Phe-46 and the *tert*-butyl portion of the molecule, respectively. Analysis of the FKBP12-**3** complex also identified possible locations for additional FKBP12-ligand hydrophobic interactions in the pyranose-binding region as described in the structure-activity section above.

Crystallographic comparison of the FKBP12-**4** and FKBP12-**3** complexes indicated that **4** bound to FKBP12 in a manner almost identical with that of **3** with the hydroxyl group oriented away from the pyranose-binding pocket toward solvent (data not shown). The reduced FKBP12 affinity of compound **4** relative to **3** presumably arises from unfavorable interactions between the polar hydroxyl group and the hydrophobic FKBP12 residues which contact both the FK506 pyranose group and the *tert*-butyl moiety of **3**. Interestingly, the electron density observed for the pyranose mimetic region of compound **4** was well-defined, in contrast to that noted for the corresponding portions of all other urea inhibitors when complexed with FKBP12. This increased definition presumably results from reduced conformational mobility imparted by the hydroxyl group of **4** and suggests that the pyranose mimics of other urea-containing FKBP12 ligands may adopt multiple binding geometries.

As was previously observed for a related  $\alpha$ -ketoamide-containing FKBP12 inhibitor, the phenethyl fragment of compound **7** interacted with FKBP12 in a region near where the cyclohexyl moiety of FK506 (C<sub>29</sub>-C<sub>34</sub>) was located in the FKBP12-FK506 crystal structure (cyclohexyl-binding region; Figure 4).<sup>20b</sup> The phenyl ring of **7** was rotated 90° relative to the plane defined by the cyclohexyl ring of FK506, presumably to maximize beneficial hydrophobic interactions with FKBP12. As was noted for compound **3** above, the benzylic ester fragment of **7** made beneficial inter- and intramolecular hydrophobic interactions with Phe-46 of FKBP12 and the *tert*-butyl pyranose mimic, respectively.

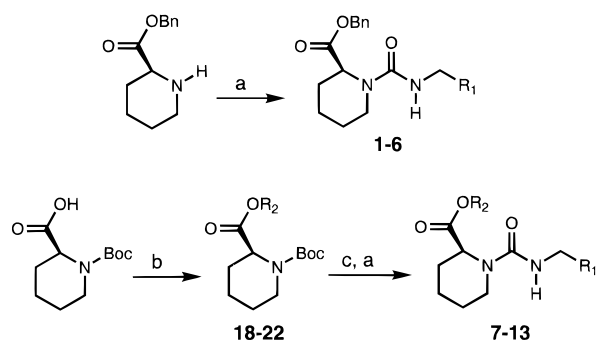
In contrast, the crystal structure of the FKBP12-**8** complex revealed that the trimethoxyphenyl fragment of **8** contacted the protein in a region occupied crystallographically by a portion of the FK506 effector domain rather than the cyclohexyl moiety as anticipated from



**Figure 5.** Crystal structure of the FKBP12-17 complex. Hydrogen bonds are indicated as white dashed lines. A portion of the water-accessible surface of the protein is shown as pink dots. Selected side chains of FKBP12 residues from the FKBP12-FK506 crystal structure are superimposed and shown in yellow.

the structure of **7** (Figure 4). Thus, a single (*meta*) aryl methoxy group interacted with FKBP12 at a site near to the location of the FK506 C<sub>19</sub> methyl group in the FKBP12-FK506 crystal structure. Good hydrophobic interactions were observed between this methoxy group (and the aryl ring itself) and Phe-46, the side chain of which was positioned as observed in the FKBP12-FK506 crystal structure. The remaining aryl methoxy groups of **8** did not appear to significantly contact FKBP12, and their removal from the inhibitor design was therefore predicted to have a negligible effect on the resulting FKBP12-ligand interactions. This prediction was verified by the preparation and analysis of compound **9** which was crystallographically observed to associate with FKBP12 in a manner similar to that described for compound **8** (data not shown). The observed binding of **8** and **9** is believed to arise from a prearrangement of the compounds in aqueous solution in which intramolecular hydrophobic interactions between the ester appendage and the pyranose mimetics are maximized.<sup>27</sup> Compound **7** may be similarly prearranged, but in this case the benzylic ester portion of the molecule contacts the *tert*-butyl pyranose mimic, allowing the phenethyl fragment to occupy the cyclohexyl-binding region of FKBP12. Similar factors may also influence the FKBP12 association of other inhibitors which contain branched pipecolyl esters derived from secondary alcohols.<sup>20</sup>

In addition to the FKBP12-acyclic urea complexes examined above, the crystal structure of the cyclic urea inhibitor **17** complexed with FKBP12 was also determined. The pipecolyl-derived portion of the 6,6-bicyclic structure was located above the indole ring of Trp-59, analogous to the positioning of the acyclic urea inhibitors examined above (Figure 5). The anticipated movement of Asp-37 away from the ligand was also observed (0.37 Å relative to its position in the FKBP12-FK506 crystal structure), presumably to accommodate the larger bicyclic structure in the FKBP12 active site. The FKBP12 residues which form hydrogen bonds to Asp-37 (Arg-42 and Tyr-26) were also slightly displaced away from the binding cavity but without significant perturbation of the general protein structure. As was noted for the acyclic ureas above, the binding geometry of the bicyclic inhibitor was significantly different from that

**Scheme 1**<sup>a</sup>

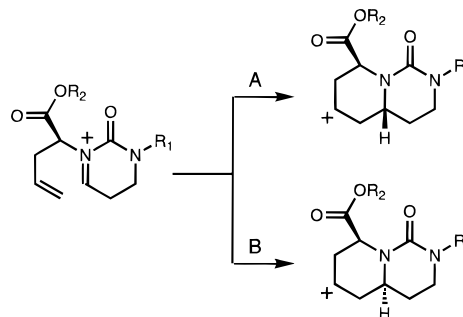
<sup>a</sup> Reagents and conditions ( $R_1$ ,  $R_2$  = see Tables 1 and 2; Bn = benzyl): (a) 1.0 equiv of  $O=C=NCH_2R_1$ , 1.0 equiv of  $Et_3N$ ,  $CH_2Cl_2$ , 23 °C, 1 h, 75–90%; (b) 1.0 equiv of  $R_2OH$ , 2.0 equiv of DCC, 0.3 equiv of CSA, 0.3 equiv of DMAP,  $CH_2Cl_2$ , 23 °C, 4–12 h, 80–90%; (c) 4.0 M HCl in 1,4-dioxane, 23 °C, 1 h.

observed for related pipecolyl-derived  $\alpha$ -ketoamides. This geometry difference was even more pronounced in the structure of **17** and caused a portion of the bicyclic structure to protrude above the FKBP12-binding pocket (Figure 5). Not unexpectedly, such binding geometry resulted in a gap between FKBP12 and the inhibitor which was larger than that detected previously for the related acyclic ureas. However, favorable hydrophobic interactions were maintained between the propyl side chain of **17** and the FKBP12 pyranose-binding residues (Phe-36, Ile-90, Ile-91, and His-87) with minimal perturbation of these residues from their observed positions in the FKBP12–FK506 crystal structure. As was noted for other benzyl pipecolyl-containing inhibitors, favorable inter- and intramolecular hydrophobic interactions were made by the benzyl ester of **17** with Phe-46 of FKBP12 and the propyl chain of the ligand, respectively.

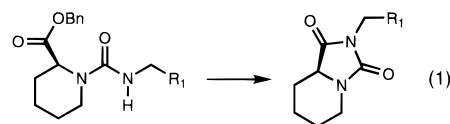
**Synthesis**

The simple benzyl pipecolyl-derived FKBP12 inhibitors were conveniently synthesized by modification of a literature procedure for the preparation of unsymmetrical ureas (Scheme 1).<sup>28</sup> Thus, appropriate primary amines were first transformed into the corresponding isocyanates by addition, with an equimolar amount of triethylamine, to a solution of triphosgene in dichloromethane at 23 °C followed by a short (~1 h) reflux period. These intermediates were not isolated but treated directly with (*S*)-pipecolic acid benzyl ester<sup>20a</sup> and an additional 1 equiv of triethylamine to provide the desired ureas in high yield (70–95%) following workup and flash column chromatography. In contrast to the related literature procedure, slow (e.g., syringe pump) addition of the primary amine substrates was not required in order to obtain good yields of the ureas. For the preparation of compound **4**, the hydroxyl group of 3-amino-2,2-dimethyl-1-propanol was converted to the corresponding *tert*-butyldimethylsilyl ether prior to urea formation. The silyl group was subsequently removed in good yield by exposure of the protected urea to triethylamine trihydrofluoride. The primary amines required for the syntheses of compounds **5** and **6** were prepared by literature methods.<sup>29</sup>

Attempted deprotection of the benzyl pipecolyl-derived ureas by a variety of methods (e.g., hydrogenation,

**Scheme 2.** Possible Cyclization Outcomes of Proposed *N*-Acyliminium Ion Intermediates in the Preparation of **14–17**

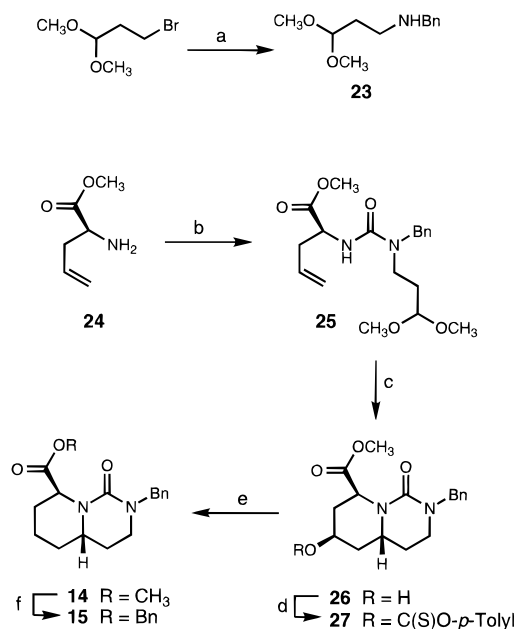
tion, basic hydrolysis) invariably resulted in the formation of the corresponding hydantoins (eq 1). Thus,



inhibitors containing ester groups other than benzyl were prepared by carbodiimide-mediated esterification of (*S*)-*N*-Boc-pipecolic acid<sup>30</sup> followed by removal of the nitrogen-protecting group and use of the resulting amine in the unsymmetrical urea synthesis described above (Scheme 1). The alcohol required for the preparation of compound **7** was synthesized by the reported literature method,<sup>20b</sup> while those utilized in the syntheses of **8** and **9** were prepared by borane-mediated reduction of the corresponding carboxylic acids.<sup>31</sup> Interestingly, all the acyclic ureas examined in the course of this work (compounds **1–13**) displayed only one significant isomer in their <sup>1</sup>H NMR spectra ( $CDCl_3$ , 23 °C). The origin of this apparent conformational bias is unknown as is the distribution of acyclic urea isomers in solvents other than chloroform (e.g., water).<sup>32</sup>

The 6,6-bicyclic molecules utilized in this study were somewhat more difficult to prepare than the acyclic ureas described above. It was envisioned that cyclization of an appropriately positioned olefin onto a transient *N*-acyliminium ion intermediate with subsequent trapping of the resulting carbocation would allow for construction of the desired 6,6-bicyclic framework (Scheme 2).<sup>33,34</sup> Examination of molecular models suggested that the cyclization which produced the undesired bicyclic structure (pathway B) would be severely disfavored by steric clashes between the ester and urea carbonyl groups relative to that which afforded the desired bicyclic framework (pathway A).<sup>33a</sup> Subsequent functional group manipulation of the cyclization product(s) would then provide the target molecules. The preparation of ureas **14** and **15** in racemic form is described below.

Treatment of 3-bromopropionaldehyde dimethyl acetal with equimolar amounts of sodium hydride and benzylamine in *N,N*-dimethylformamide at 80 °C for 5 h afforded the monoalkylation product **23** in moderate yield following workup and flash column chromatography (Scheme 3). This compound was efficiently coupled with racemic allylglycine methyl ester (**24**) utilizing the previously described method for unsymmetrical urea preparation to afford urea **25** after purification on neutral silica gel. Exposure of **25** to a 1:1 mixture of

Scheme 3<sup>a</sup>

<sup>a</sup> Reagents and conditions (Bn = benzyl): (a) 1.0 equiv of NaH, 1.0 equiv of BnNH<sub>2</sub>, DMF, 23 → 80 °C, 5 h, 36%; (b) 0.33 equiv of (Cl<sub>3</sub>CO)<sub>2</sub>CO, 1.0 equiv of Et<sub>3</sub>N, CH<sub>2</sub>Cl<sub>2</sub>, 23 → 40 °C, 1 h, then 1.0 equiv of 23, 1.0 equiv of Et<sub>3</sub>N, 15 min, 88%; (c) 1:1 TFA:CH<sub>2</sub>Cl<sub>2</sub>, 23 °C, 2 h, 71%; (d) 6.0 equiv of ClC(S)O-*p*-Tolyl, 6.5 equiv of DMAP, CH<sub>3</sub>CN, 82 °C, 10 h, 50%; (e) 1.5 equiv of (TMS)<sub>3</sub>SiH, 0.2 equiv of AIBN, toluene, 80 °C, 1 h, 91%; (f) 10 equiv of NaOH, CH<sub>3</sub>OH, 23 °C, 4 h, then 3.0 equiv of EDC, 3.0 equiv of BnOH, 0.15 equiv of DMAP, CH<sub>2</sub>Cl<sub>2</sub>, 23 °C, 1 h, 72%.

trifluoroacetic acid and dichloromethane at ambient temperature for 2 h provided the 6,6-bicyclic compound **26** in 71% yield following a basic quench and flash column chromatography. Prolonged reaction times significantly reduced the yield of the cyclic urea, and small amounts of additional uncharacterized products were formed during the cyclization reaction.<sup>35</sup> The relative stereochemistry of **26** was established by an X-ray crystal structure determination which confirmed that the desired 6,6-bicyclic ring system had been formed. In addition, the crystal structure indicated that trapping of the intermediate carbocation occurred from the same face as the ester moiety (cf. Scheme 2). It is uncertain whether the observed alcohol stereochemistry resulted from a directed intermolecular trapping event or by an intramolecular cyclization involving the ester group with subsequent methanolysis of the intermediate lactone.

Attempts to deoxygenate **26** proved troublesome, presumably due to steric effects resulting from the cis-1,3-relationship of the alcohol and ester groups. The desired transformation was eventually accomplished by reducing the corresponding thionoformate **27** with tris(trimethylsilyl)silane/AIBN to afford methyl ester **14** in moderate yield.<sup>36,37</sup> Basic hydrolysis of **14** and esterification of the resulting carboxylic acid with benzyl alcohol afforded benzyl ester **15** in good yield. The preparation of the 6,6-bicyclic-*N*-propyl compounds **16** and **17** was analogous to that described for the *N*-benzyl ureas above and proceeded through intermediates **28**–**31** (see the Experimental Section). The stereochemistry of the corresponding *N*-acyliminium ion cyclization product **30** was assigned by analogy to the *N*-benzyl series described above, and successful preparation of the

desired 6,6-bicyclic ring system was confirmed by analysis of the FKBP12–**17** crystal structure (see above).

## Conclusions

The ability of the urea functional group to replace the α-ketoamide moiety present in potent FKBP12-binding molecules was demonstrated by the synthesis and biological evaluation of several acyclic and cyclic urea-containing compounds. Such molecules disrupted FKBP12 isomerase activity with apparent inhibition constants (*K<sub>i,app</sub>*) approaching 0.10 μM. X-ray crystallographic analysis of several ureas complexed with FKBP12 established that the compounds associated with the protein in a manner similar to, but significantly different from, that observed for related α-ketoamide-containing FKBP12 inhibitors (including the natural product FK506). The crystal structures also provided insight for the possible extension of the simple FKBP12-binding domains to include additional functionality necessary to impart immunosuppressive properties to this class of compounds.

## Experimental Section

**General.** All reactions were performed in septum-sealed flasks under a slight positive pressure of argon unless otherwise noted. All commercial reagents and solvents were used as received from their respective suppliers with the following exceptions. Tetrahydrofuran (THF) was distilled from sodium benzophenone ketyl prior to use. Dichloromethane (CH<sub>2</sub>Cl<sub>2</sub>) was distilled from calcium hydride prior to use. 2,2,2-Trifluoroethanol was distilled from sodium prior to use. The succinyl-Ala-Leu-Pro-Phe-*p*-nitroanilide peptide used in enzyme assays was purchased from Bachem. Flash column chromatography<sup>38</sup> was performed using silica gel 60 (Merck art. 9385). <sup>1</sup>H NMR spectra were recorded at 300 MHz utilizing either a Varian UNITYplus 300 or a General Electric QE-300 spectrometer. Chemical shifts are reported in ppm (δ) downfield relative to internal tetramethylsilane, and coupling constants are given in Hertz. Infrared absorption spectra were recorded using a Perkin-Elmer 1600 series FTIR spectrometer. Continuous spectrophotometric enzyme assays were performed using either a Beckman DU-12 or a Perkin-Elmer Lambda 2 spectrophotometer. Elemental analyses were performed by Atlantic Microlab, Inc., Norcross, GA. Melting points are uncorrected.

**Protein–Ligand Crystal Structure Determination.** Wild-type human FKBP12 and an FKBP12 mutant (R13Q, K17Q, K92Q) designed to facilitate crystallization were expressed in *Escherichia coli* and purified according to standard procedures<sup>39</sup> with the following modifications: Cells were disrupted by microfluidization (Microfluidics Corp. Model M110Y), a fast flow DEAE Sepharose (Pharmacia) column was used instead of a DE-52 (Whatman) column, and two ammonium sulfate cuts (46% with retention of supernatant, 86% with retention of pellet) replaced the heat treatment step. Samples of the ligands were dissolved in DMSO at a concentration of 0.5 M and mixed in a 5:1 molar ratio with wild-type (compounds **3**, **4**, **7**, and **17**) or mutant (compounds **8** and **9**) FKBP12. The FKBP12–ligand complexes were spun on a desktop centrifuge at 15 000 rpm for 5 min to remove particulates prior to use.

Crystals of the complexes were obtained by vapor diffusion at room temperature. A given solution of FKBP12–ligand complex (3 μL) was mixed with reservoir solution (3 μL) to form the required hanging drops. Crystals of the complexes were obtained using the following reservoir solutions: 2% poly(ethylene glycol) 400, 1.4 M Na/K phosphate, pH 7.5 (FKBP12–**3**); 2.0 M sodium formate, 0.1 M bis-Tris, pH 6.0 (FKBP12–**4**); 1.0 M sodium formate, 0.1 M HEPES, pH 7.0 (FKBP12–**7**); 1.4 M Na/K phosphate, 0.1 M cacodylate, pH 6.5 (FKBP12–**8**); 1.4 M ammonium phosphate, 0.1 M bis-Tris, pH 5.5



**Table 5.** X-ray Data Collection and Refinement Statistics for FKBP12–Ligand Complexes

	<b>3</b>	<b>4</b>	<b>7</b>	<b>8</b>	<b>9</b>	<b>17</b>
cell constants (Å):						
<i>a</i>	31.47	31.36	31.52	33.46	33.25	31.44
<i>b</i>	43.10	43.61	43.66	36.59	36.44	43.39
<i>c</i>	77.76	77.79	77.77	92.51	93.37	77.66
data collection:						
no. observations	25 848	30 819	28 315	34 598	17 242	44 047
no. unique reflections	9029	12 282	9526	10 231	6639	9920
resolution range (Å)	20–1.8	20–1.65	20–1.8	20–1.8	20–2.1	20–1.8
<i>R</i> <sub>sym</sub> <sup>a</sup>	0.051	0.031	0.058	0.034	0.064	0.064
completeness	0.88	0.92	0.93	0.92	0.94	0.96
refinement:						
resolution range (Å)	10–1.8	10–1.65	10–1.8	10–1.8	10–2.1	10–1.8
final <i>R</i> factor <sup>b</sup>	0.173	0.185	0.190	0.192	0.184	0.179
rms bond dev (Å)	0.014	0.013	0.014	0.015	0.016	0.014
rms angle dev (deg)	2.62	2.73	2.65	2.96	2.95	2.67
av <i>B</i> , protein (Å <sup>2</sup> )	9.33	12.73	10.75	26.17	30.49	13.20
av <i>B</i> , ligand (Å <sup>2</sup> )	10.18	12.88	11.98	20.69	21.97	15.02
no. solvent molecules	115	72	120	63	37	85

<sup>a</sup>  $\sum_h \sum_i |I_{h,i} - \bar{I}_h| / \sum_h \sum_i I_{h,i}$  where  $\langle I_h \rangle$  is the mean intensity for the *i* observations of reflection *h*. <sup>b</sup>  $\sum |F_o - F_c| / \sum F_o$ , where *F*<sub>o</sub> and *F*<sub>c</sub> are the observed and calculated structure factor amplitudes, respectively.

(FKBP12–**9**); and 1.5 M ammonium sulfate, 0.1 M cacodylate, pH 6.5 (FKBP12–**17**).

All X-ray data sets (Table 5) were collected at room temperature using a San Diego Multiwire Systems area detector with a Rigaku RU-200 copper rotating anode operating at 50 kV and 180 mA. Crystals of complexes formed with wild-type FKBP12 grew in space group *P*2<sub>1</sub>2<sub>1</sub>2<sub>1</sub> with one complex in the asymmetric unit. Crystals of complexes formed with the mutant FKBP12 grew in space group *P*2<sub>1</sub>2<sub>1</sub>2<sub>1</sub> with altered cell dimensions and also contained one complex per asymmetric unit.

The structure of the FKBP12–**3** complex was determined by molecular replacement using the protein coordinates from the FKBP12–FK506 crystal structure as a search model.<sup>15</sup> Molecular replacement and refinement calculations were carried out using the program X-PLOR.<sup>40</sup> A cross-rotation search was performed in 2.5° intervals using 15–4 Å resolution data and a maximum cross-vector length of 40 Å. The rotation corresponding to the highest peak in the search (6.4σ) was optimized by Patterson correlation refinement and used to generate starting coordinates for the translation search. A translation search over a 1.0 Å grid using 15–3 Å resolution data produced a clear solution (peak height of 13.8σ). The resulting model produced an *R*-factor of 0.379 for data (*F* > 2σ<sub>F</sub>) in the resolution range 10–3.0 Å after rigid-body refinement. The model was refined with the simulated annealing and conjugate gradient minimization protocols in X-PLOR using all data in the 10–1.8 Å resolution range. A model of **3**, constructed using the program Quanta,<sup>41</sup> was then fit to a difference electron density map, and the combined model was refined.

Structures of FKBP12 complexed with compounds **4**, **7**, and **17** were determined using the protein coordinates from the FKBP12–**3** complex crystal structure as a starting model. In each case, the ligand was fit to a difference electron density map after initial refinement of the protein coordinates. The structure of the FKBP12–**8** complex was determined by molecular replacement using the coordinates of FKBP12 from the FKBP12–**4** complex structure as a search model. The rotation corresponding to the highest peak (6.8σ) in a cross-rotation search using 15–4 Å data was optimized by Patterson correlation refinement and used to generate starting coordinates for the translation search. The translation function solution (peak height of 11.9σ) produced a model with an *R*-factor of 0.341 for all data in the resolution range 10–3.0 Å after rigid-body refinement. This model was refined with the conjugate gradient minimization protocol in X-PLOR using all data in the 10–1.8 Å resolution range, and a model of **8** was fit to a difference electron density map. The structure of the FKBP12–**9** complex was determined using the protein coordinates from the FKBP12–**8** complex crystal structure as the

starting model. After initial refinement of the protein coordinates, a model of **9** was fit to a difference electron density map.

Refinement of all FKBP12–ligand complexes was performed using a combination of simulated annealing and conventional positional refinement along with refinement of individual atomic temperature factors. The structures were checked and corrected using a series of simulated-annealing omit maps. Display of electron density and manual adjustment of the model were performed using the program X-FIT.<sup>42</sup> Water molecules were assigned to 4σ peaks in difference electron density maps when there was good hydrogen-bond geometry to protein atoms. Refinement results are summarized in Table 5.

**Enzyme Assays.** Wild-type human recombinant FKBP12 was purified as described above. Peptidylprolyl isomerase activity was determined spectrophotometrically as described using 100 μM succinyl-Ala-Leu-Pro-Phe-*p*-nitroanilide as a substrate.<sup>43</sup> The substrate was dried in vacuo over P<sub>2</sub>O<sub>5</sub> at room temperature, dissolved in 2,2,2-trifluoroethanol containing 240 mM LiCl, and subsequently stored under argon at –20 °C. The percentage of *cis*-succinyl-Ala-Leu-Pro-Phe-*p*-nitroanilide present in the equilibrium mixture was usually about 45%, allowing significant portions of the reaction progress curves to be obtained. Continuous spectrophotometric assays were performed at 10 or 15 °C in the presence of 50 mM HEPES (pH 8.0), 100 mM NaCl, 100 μM 2-mercaptoethanol, 1% 2,2,2-trifluoroethanol, 2.5 mM LiCl, 1% DMSO, 90 nM FKBP12, 100 μM *cis*-peptide substrate, and 6 mg/mL α-chymotrypsin coupling enzyme. Data for reaction progress curves were collected for 5 min, and initial velocities were determined by nonlinear least-squares fits of each progress curve to a single exponential. Apparent *K*<sub>i</sub>'s were determined by analyzing the concentration dependence of each inhibitor on prolyl isomerase activity compared to a control that contained all components of the reaction mixture except inhibitor. These data were fit to an equation for competitive tight-binding inhibition with a correction for uncatalyzed isomerization. Standard errors for the fit data were <1%. All data were analyzed using the software program KineTic (BioKin, Ltd., Madison, WI). The *k*<sub>cat</sub> and *K*<sub>m</sub> values determined for the succinyl-Ala-Leu-Pro-Phe-*p*-nitroanilide substrate, purified recombinant FKBP12, and FKBP12 mutant were similar to those reported previously.<sup>43</sup> Using these methods, *K*<sub>i,app</sub>'s of 0.28 nM for FK506 and 0.20 nM for rapamycin were measured in agreement with previous reports.<sup>43,44</sup>

**Representative Procedure for Synthesis of Acyclic Ureas 1–6. (2*S*)-1-[(2-Methylallyl)carbamoyl]piperidine-2-carboxylic Acid Benzyl Ester (**1**).** A solution of 2-methylallylamine (0.099 g, 1.39 mmol, 1 equiv) and Et<sub>3</sub>N (0.194 mL, 1.39 mmol, 1.0 equiv) in CH<sub>2</sub>Cl<sub>2</sub> (3 mL) was added over 2 min to a solution of triphosgene (0.137 g, 0.462 mmol, 0.33



equiv) in  $\text{CH}_2\text{Cl}_2$  (5 mL) at 23 °C. The resulting mixture was refluxed for 1 h and then cooled to 23 °C. A solution of (2*S*)-piperidine-2-carboxylic acid benzyl ester<sup>20a</sup> (0.306 g, 1.39 mmol, 1.0 equiv) and  $\text{Et}_3\text{N}$  (0.194 mL, 1.39 mmol, 1.0 equiv) in  $\text{CH}_2\text{Cl}_2$  (5 mL) was then added over 5 min. The mixture was stirred at 23 °C for 1 h and then partitioned between water (100 mL) and a 1:1 mixture of EtOAc and hexanes (2 × 100 mL). The combined organic layers were dried over  $\text{Na}_2\text{SO}_4$  and concentrated. Purification of the residue by flash column chromatography (40% EtOAc in hexanes) afforded urea **1** (0.320 g, 73%) as a colorless oil:  $R_f$  = 0.45 (50% EtOAc in hexanes); IR ( $\text{cm}^{-1}$ ) 3354, 1738, 1630;  $^1\text{H}$  NMR ( $\text{CDCl}_3$ , major isomer)  $\delta$  1.19–1.28 (m, 1 H), 1.42–1.56 (m, 1 H), 1.65–1.71 (m, 2 H), 1.73 (s, 3 H), 2.26 (d, 1 H,  $J$  = 14.0), 3.17 (td, 1 H,  $J$  = 12.2, 3.2), 3.50–3.55 (m, 1 H), 3.80 (d, 2 H,  $J$  = 5.6), 4.71–4.74 (m, 1 H), 4.80 (s, 1 H), 4.83 (s, 1 H), 5.11–5.12 (m, 1 H), 5.12 (d, 1 H,  $J$  = 12.4), 5.19 (d, 1 H,  $J$  = 12.4), 7.28–7.38 (m, 5 H). Anal. ( $\text{C}_{18}\text{H}_{24}\text{N}_2\text{O}_3$ ) C, H, N.

**(2*S*)-1-[(2*S*)-piperidine-2-carboxylic acid benzyl ester (2):**  $R_f$  = 0.21 (30% EtOAc in hexanes); IR ( $\text{cm}^{-1}$ ) 3355, 1737, 1711, 1631;  $^1\text{H}$  NMR ( $\text{CDCl}_3$ )  $\delta$  0.82–0.90 (m, 1 H), 1.19–1.28 (m, 1 H), 1.41–1.50 (m, 1 H), 1.65–1.76 (m, 2 H), 2.24–2.29 (m, 1 H), 3.15 (td, 1 H,  $J$  = 12.3, 3.0), 3.47–3.52 (m, 1 H), 4.42–4.45 (m, 2 H), 4.89 (t, 1 H,  $J$  = 4.9), 5.12–5.13 (m, 1 H), 5.13 (d, 1 H,  $J$  = 12.4), 5.20 (d, 1 H,  $J$  = 12.4), 7.24–7.40 (m, 10 H). Anal. ( $\text{C}_{21}\text{H}_{24}\text{N}_2\text{O}_3$ ) C, H, N.

**(2*S*)-1-[(2*S*)-piperidine-2-carboxylic acid benzyl ester (3):**  $R_f$  = 0.31 (30% EtOAc in hexanes); IR ( $\text{cm}^{-1}$ ) 3365, 1739, 1632;  $^1\text{H}$  NMR ( $\text{CDCl}_3$ , major isomer)  $\delta$  0.88 (s, 9 H), 1.42–1.57 (m, 1 H), 1.63–1.77 (m, 3 H), 2.20–2.28 (m, 1 H), 3.00–3.21 (m, 3 H), 3.47–3.52 (m, 1 H), 4.60–4.64 (m, 1 H), 5.08–5.10 (m, 1 H), 5.12 (d, 1 H,  $J$  = 12.6), 5.18 (d, 1 H,  $J$  = 12.6), 7.28–7.37 (m, 5 H). Anal. ( $\text{C}_{19}\text{H}_{28}\text{N}_2\text{O}_3$ ) C, H, N.

**(2*S*)-1-[(3'-Hydroxy-2',2'-dimethylpropyl)carbamoyl]-piperidine-2-carboxylic Acid Benzyl Ester (4):** *tert*-Butyldimethylsilyl chloride (12.50 g, 83.1 mmol, 1.0 equiv),  $\text{Et}_3\text{N}$  (12.71 mL, 91.0 mmol, 1.1 equiv), and DMAP (0.10 g, 0.83 mmol, 0.01 equiv) were added sequentially to a solution of 2,2-dimethyl-3-aminopropanol (8.56 g, 83.1 mmol, 1.0 equiv) in  $\text{CH}_2\text{Cl}_2$  (100 mL) at 0 °C. The resulting mixture was maintained at 0 °C for 2 h and then partitioned between water (150 mL) and  $\text{CH}_2\text{Cl}_2$  (2 × 50 mL). The combined organic layers were washed sequentially with water (100 mL) and brine (100 mL) and then dried over  $\text{Na}_2\text{SO}_4$  and concentrated. The residue was purified by flash column chromatography (gradient elution 10% → 40% EtOAc in hexanes) to afford 3-[(*tert*-butyldimethylsilyl)oxy]-2,2-dimethylpropylamine (15.20 g, 84.1%) as a clear oil:  $R_f$  = 0.30 (50% EtOAc in hexanes); IR ( $\text{cm}^{-1}$ ) 3319;  $^1\text{H}$  NMR ( $\text{CDCl}_3$ )  $\delta$  0.03 (s, 6 H), 0.79 (s, 6 H), 0.86 (s, 9 H), 1.10 (s, br, 2 H), 2.49 (s, 2 H), 3.28 (s, 2 H). Anal. Calcd for  $\text{C}_{11}\text{H}_{27}\text{NOSi}$ : C, 60.77; H, 12.52; N, 6.44. Found: C, 61.02; H, 12.37; N, 6.32.

The urea derived from (2*S*)-piperidine-2-carboxylic acid benzyl ester<sup>20a</sup> and 3-[(*tert*-butyldimethylsilyl)oxy]-2,2-dimethylpropylamine was prepared utilizing the general procedure described above:  $R_f$  = 0.68 (40% EtOAc in hexanes); IR ( $\text{cm}^{-1}$ ) 3371, 1740, 1632;  $^1\text{H}$  NMR ( $\text{CDCl}_3$ , major isomer)  $\delta$  0.53 (s, 6 H), 0.82 (s, 3 H), 0.84 (s, 3 H), 0.85 (s, 9 H), 1.23–1.62 (m, 8 H), 2.25 (m, 1 H), 3.19 (m, 2 H), 3.46 (s, 2 H), 5.02 (s, br, 1 H), 5.11 (d, 1 H,  $J$  = 12.3), 5.19 (d, 1 H,  $J$  = 12.3), 5.51 (t, 1 H,  $J$  = 6.1), 7.29 (s, 5 H). Anal. Calcd for  $\text{C}_{25}\text{H}_{42}\text{N}_2\text{O}_4\text{Si}$ : C, 64.90; H, 9.15; N, 6.05. Found: C, 64.78; H, 9.18; N, 5.98.

Triethylamine trihydrofluoride (0.60 mL) was added to a solution of this urea (0.041 g, 0.09 mmol) in THF (3 mL) at 23 °C. The reaction mixture was stirred at 23 °C for 4 h and then partitioned between water (50 mL) and EtOAc (2 × 50 mL). The combined organic layers were washed with brine (50 mL) and then dried over  $\text{Na}_2\text{SO}_4$  and concentrated. The residue was purified by flash column chromatography (30% EtOAc in hexanes) to afford urea **4** (0.024 g, 76%) as a colorless oil:  $R_f$  = 0.31 (40% EtOAc in hexanes); IR ( $\text{cm}^{-1}$ ) 3354, 1738, 1621;  $^1\text{H}$  NMR ( $\text{CDCl}_3$ , major isomer)  $\delta$  0.82 (s, 3 H), 0.85 (s, 3 H), 1.19–1.75 (m, 8 H), 2.25 (m, 1 H), 2.92–3.25 (m, 4 H), 4.41 (t, 1 H,  $J$  = 7.3), 4.99 (m, 1 H), 5.21 (s, 2 H), 7.33 (s, 5 H). Anal. ( $\text{C}_{19}\text{H}_{28}\text{N}_2\text{O}_4$ ) C, H, N.

**(2*S*)-1-[(1'-Methylcyclopentyl)methyl]carbamoyl]-piperidine-2-carboxylic acid benzyl ester (5):**  $R_f$  = 0.35 (40% EtOAc in hexanes); IR ( $\text{cm}^{-1}$ ) 3364, 1738, 1631;  $^1\text{H}$  NMR ( $\text{CDCl}_3$ , major isomer)  $\delta$  0.95 (s, 3 H), 1.25–1.56 (m, 10 H), 2.24 (s, br, 2 H), 3.18 (m, 3 H), 3.50 (m, 1 H), 3.75 (m, 1 H), 4.28 (m, 1 H), 4.62 (t, 1 H,  $J$  = 5.9), 5.05 (m, 1 H), 5.12 (d, 1 H,  $J$  = 12.5), 5.18 (d, 1 H,  $J$  = 12.4), 7.36 (s, 5 H). Anal. ( $\text{C}_{21}\text{H}_{30}\text{N}_2\text{O}_3$ ) C, H, N.

**(2*S*)-1-[(1'-Methylcyclohexyl)methyl]carbamoyl]-piperidine-2-carboxylic acid benzyl ester (6):**  $R_f$  = 0.66 (5%  $\text{CH}_3\text{OH}$  in  $\text{CH}_2\text{Cl}_2$ ); IR ( $\text{cm}^{-1}$ ) 3362, 1739, 1631;  $^1\text{H}$  NMR ( $\text{CDCl}_3$ , major isomer)  $\delta$  0.84 (s, 3 H), 1.17–1.30 (m, 6 H), 1.34–1.54 (m, 6 H), 1.60–1.73 (m, 3 H), 2.18–2.26 (m, 1 H), 3.06 (dd, 1 H,  $J$  = 13.5, 5.9), 3.10–3.20 (m, 2 H), 3.43–3.51 (m, 1 H), 4.56–4.62 (m, 1 H), 5.04–5.08 (m, 1 H), 5.12 (d, 1 H,  $J$  = 12.4), 5.18 (d, 1 H,  $J$  = 12.4), 7.29–7.34 (m, 5 H). Anal. ( $\text{C}_{22}\text{H}_{32}\text{N}_2\text{O}_3$ ) C, H, N.

**Representative Procedure for Esterification of (S)-N-Boc-pipecolinic Acid. (2*S*)-Piperidine-1,2-dicarboxylic Acid 1-*tert*-Butyl 2-[(1'*R*)-1',3'-Diphenylpropyl] Diester (18).** 1-[3-(Dimethylamino)propyl]-3-ethylcarbodiimide hydrochloride (0.418 g, 2.18 mmol, 1.5 equiv) and DMAP (0.025 g, 0.21 mmol, 0.14 equiv) were added sequentially to a solution of (1'*R*)-1,3-diphenylpropanol<sup>20b</sup> (0.309 g, 1.46 mmol, 1 equiv) and (S)-N-Boc-pipecolinic acid<sup>30</sup> (0.500 g, 2.18 mmol, 1.5 equiv) in  $\text{CH}_2\text{Cl}_2$  (10 mL) at 23 °C. The resulting solution was stirred for 3 h at 23 °C and then partitioned between water (100 mL) and a 1:1 mixture of EtOAc and hexanes (2 × 100 mL). The combined organic layers were dried over  $\text{Na}_2\text{SO}_4$  and concentrated. The residue was purified by flash column chromatography (5% EtOAc in hexanes) to provide ester **18** (0.574 g, 93%) as a colorless oil:  $R_f$  = 0.74 (20% EtOAc in hexanes); IR ( $\text{cm}^{-1}$ ) 1739, 1695;  $^1\text{H}$  NMR ( $\text{CDCl}_3$ , 1:1 mixture of isomers)  $\delta$  1.05–1.29 (m, 1.34 (s), 1.37–1.43 (m), 1.48 (s), 1.59–1.72 (m), 2.03–2.34 (m), 2.53–2.69 (m), 2.81–2.98 (m), 3.91–4.05 (m), 4.74–4.75 (m), 4.96–4.97 (m), 5.80 (dd,  $J$  = 7.7, 5.8), 7.08–7.39 (m). Anal. ( $\text{C}_{26}\text{H}_{33}\text{NO}_4$ ) C, H, N.

**(2*S*)-Piperidine-1,2-dicarboxylic acid 1-*tert*-butyl 2-[3'-(3,4,5-trimethoxyphenyl)propyl] diester (19):**  $R_f$  = 0.65 (50% EtOAc in hexanes); IR ( $\text{cm}^{-1}$ ) 1738, 1694;  $^1\text{H}$  NMR ( $\text{CDCl}_3$ , 1:1 mixture of isomers)  $\delta$  0.86–0.89 (m), 1.20–1.38 (m), 1.62–1.74 (m), 2.20–2.24 (m), 2.63 (t,  $J$  = 7.6), 2.84–3.03 (m), 3.83 (s), 3.85 (s), 4.11–4.17 (m), 4.75 (s, br), 4.91 (s, br), 6.40 (s). Anal. ( $\text{C}_{23}\text{H}_{35}\text{NO}_7$ ) C, H, N.

**(2*S*)-Piperidine-1,2-dicarboxylic acid 1-*tert*-butyl 2-[3'-(3-methoxyphenyl)propyl] diester (20):**  $R_f$  = 0.60 (30% EtOAc in hexanes); IR ( $\text{cm}^{-1}$ ) 1739, 1696;  $^1\text{H}$  NMR ( $\text{CDCl}_3$ , 1:1 mixture of isomers)  $\delta$  1.21–1.40 (m), 1.45 (s), 1.47 (s), 1.53–1.72 (m), 1.92–2.01 (m), 2.17–2.24 (m), 2.67 (t,  $J$  = 7.8), 2.88–2.98 (m), 3.80 (s), 3.92–4.08 (m), 4.16 (t,  $J$  = 6.4), 4.74–4.76 (m), 4.90–4.91 (m), 6.73–7.18 (m), 7.19–7.23 (m). Anal. ( $\text{C}_{21}\text{H}_{31}\text{NO}_5$ ) C, H, N.

**(2*S*)-Piperidine-1,2-dicarboxylic acid 1-*tert*-butyl 2-[3'-(phenoxybenzyl) diester (21):**  $R_f$  = 0.65 (30% EtOAc in hexanes); IR ( $\text{cm}^{-1}$ ) 1742, 1697;  $^1\text{H}$  NMR ( $\text{CDCl}_3$ , mixture of isomers)  $\delta$  0.86–0.91 (m), 0.96–1.27 (m), 1.38 (s), 1.45 (s), 1.56–1.73 (m), 2.17–2.20 (m), 2.86–2.98 (m), 3.88–4.03 (m), 4.75 (s, br), 4.94 (s, br), 5.07–5.20 (m), 6.91–7.14 (m), 7.23–7.38 (m). Anal. ( $\text{C}_{24}\text{H}_{29}\text{NO}_5$ ) C, H, N.

**(2*S*)-Piperidine-1,2-dicarboxylic acid 1-*tert*-butyl 2-(4'-phenylbutyl) diester (22):**  $R_f$  = 0.68 (30% EtOAc in hexanes); IR ( $\text{cm}^{-1}$ ) 1739, 1698;  $^1\text{H}$  NMR ( $\text{CDCl}_3$ , 1:1 mixture of isomers)  $\delta$  1.13–1.35 (m), 1.42 (s), 1.45 (s), 1.52–1.75 (m), 2.17–2.19 (m), 2.61–2.66 (m), 2.81–2.99 (m), 3.89–4.08 (m), 4.15 (s, br), 4.70 (s, br), 4.87 (s, br), 7.15–7.20 (m), 7.23–7.30 (m). Anal. ( $\text{C}_{21}\text{H}_{31}\text{NO}_4$ ) C, H, N.

**Representative Procedure for the Synthesis of Acyclic Ureas 7–13. (2*S*)-1-[(2',2'-Dimethylpropyl)carbamoyl]-piperidine-2-carboxylic Acid (1'*R*)-1',3'-Diphenylpropyl Ester (7).** A solution of HCl in 1,4-dioxane (4.0 M, 2.0 mL) was added to a solution of **18** (0.570 g, 1.35 mmol) in the same solvent (2 mL) at 23 °C. The reaction mixture was stirred for 2 h at 23 °C and then carefully partitioned between saturated  $\text{NaHCO}_3$  (100 mL) and EtOAc (3 × 100 mL). The combined organic layers were dried over  $\text{Na}_2\text{SO}_4$  and concentrated to afford the crude amine product (0.383 g, 88%). The free amine

thus obtained was immediately coupled with 2,2-dimethylpropylamine utilizing the procedure described above for the preparation of compounds **1–6** to afford urea **7** (77%) as a colorless oil:  $R_f$  = 0.30 (30% EtOAc in hexanes); IR ( $\text{cm}^{-1}$ ) 3356, 1734, 1627;  $^1\text{H}$  NMR ( $\text{CDCl}_3$ , major isomer)  $\delta$  0.88 (s, 9 H), 1.05–1.32 (m, 1 H), 1.43–1.57 (m, 1 H), 1.68–1.79 (m, 3 H), 2.02–2.14 (m, 1 H), 2.19–2.32 (m, 2 H), 2.51–2.69 (m, 2 H), 3.00 (dd, 1 H,  $J$  = 13.3, 5.8), 3.07–3.18 (m, 2 H), 3.54 (dd, 1 H,  $J$  = 12.1, 3.2), 4.59 (t, 1 H,  $J$  = 5.9), 5.06–5.08 (m, 1 H), 5.79 (dd, 1 H,  $J$  = 7.6, 6.0), 7.13–7.20 (m, 4 H), 7.24–7.34 (m, 6 H). Anal. ( $\text{C}_{27}\text{H}_{36}\text{N}_2\text{O}_3$ ) C, H, N.

**(2*S*)-1-[(2',2'-Dimethylpropyl)carbamoyl]piperidine-2-carboxylic acid 3''-(3,4,5-trimethoxyphenyl)propyl ester (8):**  $R_f$  = 0.31 (50% EtOAc in hexanes); IR ( $\text{cm}^{-1}$ ) 3371, 1736, 1633;  $^1\text{H}$  NMR ( $\text{CDCl}_3$ , major isomer)  $\delta$  0.91 (s, 9 H), 1.24–1.31 (m, 1 H), 1.49–1.57 (m, 1 H), 1.67–1.78 (m, 3 H), 1.91–2.00 (m, 2 H), 2.18–2.25 (m, 1 H), 2.62 (t, 2 H,  $J$  = 7.7), 3.04 (dd, 1 H,  $J$  = 13.4, 6.0), 3.12 (dd, 1 H,  $J$  = 13.4, 6.3), 3.21 (td, 1 H,  $J$  = 12.1, 3.3), 3.48–3.53 (m, 1 H), 3.83 (s, 3 H), 3.85 (s, 6 H), 4.15 (t, 2 H,  $J$  = 6.5), 4.65 (t, 1 H,  $J$  = 5.9), 5.04–5.05 (m, 1 H), 6.39 (s, 2 H). Anal. ( $\text{C}_{24}\text{H}_{38}\text{N}_2\text{O}_6$ ) C, H, N.

**(2*S*)-1-[(2',2'-Dimethylpropyl)carbamoyl]piperidine-2-carboxylic acid 3''-(3-methoxyphenyl)propyl ester (9):**  $R_f$  = 0.23 (30% EtOAc in hexanes); IR ( $\text{cm}^{-1}$ ) 3365, 1737, 1626;  $^1\text{H}$  NMR ( $\text{CDCl}_3$ , major isomer)  $\delta$  0.90 (s, 9 H), 1.49–1.55 (m, 1 H), 1.67–1.77 (m, 3 H), 1.91–2.00 (m, 2 H), 2.21–2.25 (m, 1 H), 2.66 (t, 2 H,  $J$  = 7.7), 2.98 (d, 1 H,  $J$  = 6.3), 3.04 (dd, 1 H,  $J$  = 13.3, 6.1), 3.12 (dd, 1 H,  $J$  = 13.3, 6.0), 3.19 (td, 1 H,  $J$  = 12.1, 3.1), 3.49–3.54 (m, 1 H), 3.80 (s, 3 H), 4.11–4.16 (m, 2 H), 4.64 (t, 1 H,  $J$  = 5.8), 5.03–5.04 (m, 1 H), 6.73–6.78 (m, 3 H), 7.18–7.23 (m, 1 H). Anal. ( $\text{C}_{22}\text{H}_{34}\text{N}_2\text{O}_4$ ) C, H, N.

**(2*S*)-1-[(2',2'-Dimethylpropyl)carbamoyl]piperidine-2-carboxylic acid 3-phenoxybenzyl ester (10):**  $R_f$  = 0.30 (30% EtOAc in hexanes); IR ( $\text{cm}^{-1}$ ) 3365, 1740, 1632;  $^1\text{H}$  NMR ( $\text{CDCl}_3$ , major isomer)  $\delta$  0.88 (s, 9 H), 1.09–1.27 (m, 1 H), 1.43–1.48 (m, 1 H), 1.50–1.57 (m, 1 H), 1.61–1.76 (m, 2 H), 2.19–2.25 (m, 1 H), 2.99–3.19 (m, 3 H), 3.32–3.48 (m, 1 H), 4.62 (t, 1 H,  $J$  = 5.9), 5.06–5.10 (m, 2 H), 5.16 (d, 1 H,  $J$  = 12.8), 6.93–7.15 (m, 5 H), 7.26–7.38 (m, 4 H). Anal. ( $\text{C}_{25}\text{H}_{32}\text{N}_2\text{O}_4$ ) C, H, N.

**(2*S*)-1-[(2',2'-Dimethylpropyl)carbamoyl]piperidine-2-carboxylic acid 4''-phenylbutyl ester (11):**  $R_f$  = 0.25 (30% EtOAc in hexanes); IR ( $\text{cm}^{-1}$ ) 3364, 1736, 1631;  $^1\text{H}$  NMR ( $\text{CDCl}_3$ , major isomer)  $\delta$  0.90 (s, 9 H), 1.22–1.31 (m, 2 H), 1.47–1.54 (m, 1 H), 1.64–1.74 (m, 5 H), 2.19–2.24 (m, 1 H), 2.62–2.66 (m, 2 H), 3.05–3.11 (m, 3 H), 3.17 (td, 1 H,  $J$  = 12.1, 2.9), 3.48–3.52 (m, 1 H), 4.13–4.15 (m, 2 H), 4.62 (t, 1 H,  $J$  = 5.4), 5.02 (d, 1 H,  $J$  = 3.3), 7.16–7.21 (m, 3 H), 7.26–7.31 (m, 2 H). Anal. ( $\text{C}_{28}\text{H}_{34}\text{N}_2\text{O}_5$ ) C, H, N.

**(2*S*)-1-[(1'-Methylcyclohexyl)methyl]carbamoyl]piperidine-2-carboxylic acid 3-phenoxybenzyl ester (12):**  $R_f$  = 0.13 (20% EtOAc in hexanes); IR ( $\text{cm}^{-1}$ ) 3357, 1741, 1632;  $^1\text{H}$  NMR ( $\text{CDCl}_3$ , major isomer)  $\delta$  0.85 (s, 3 H), 1.14–1.34 (m, 6 H), 1.35–1.58 (m, 6 H), 1.60–1.77 (m, 3 H), 2.16–2.25 (m, 1 H), 3.04 (dd, 1 H,  $J$  = 13.4, 5.9), 3.08–3.21 (m, 2 H), 3.42–3.50 (m, 1 H), 4.55–4.62 (m, 1 H), 5.05–5.12 (m, 2 H), 5.15 (d, 1 H,  $J$  = 12.4), 6.92–7.15 (m, 6 H), 7.25–7.37 (m, 3 H). Anal. ( $\text{C}_{28}\text{H}_{36}\text{N}_2\text{O}_4$ ) C, H, N.

**(2*S*)-1-[(1'-Methylcyclohexyl)methyl]carbamoyl]piperidine-2-carboxylic acid 4''-phenylbutyl ester (13):**  $R_f$  = 0.66 (5%  $\text{CH}_3\text{OH}$  in  $\text{CH}_2\text{Cl}_2$ ); IR ( $\text{cm}^{-1}$ ) 3372, 1738, 1631;  $^1\text{H}$  NMR ( $\text{CDCl}_3$ , major isomer)  $\delta$  0.87 (s, 3 H), 1.21–1.33 (m, 6 H), 1.35–1.56 (m, 6 H), 1.62–1.75 (m, 7 H), 2.16–2.24 (m, 1 H), 2.60–2.66 (m, 2 H), 3.05 (dd, 1 H,  $J$  = 13.4, 5.9), 3.10–3.21 (m, 2 H), 3.45–3.53 (m, 1 H), 4.10–4.16 (m, 2 H), 4.56–4.61 (m, 1 H), 4.98–5.02 (m, 1 H), 7.14–7.21 (m, 3 H), 7.25–7.31 (m, 2 H). Anal. ( $\text{C}_{25}\text{H}_{38}\text{N}_2\text{O}_3$ ) C, H, N.

**Benzyl(3,3-dimethoxypropyl)amine (23).** Sodium hydride (0.983 g of a 60% dispersion in mineral oil, 24.6 mmol, 1.0 equiv) and 3-bromopropionaldehyde dimethyl acetal (5.0 g, 24.6 mmol, 1.0 equiv) were added sequentially to a solution of benzylamine (2.69 mL, 24.6 mmol, 1 equiv) in DMF (60 mL) at 23 °C. The resulting suspension was stirred for 3 h at 23 °C and then maintained at 80 °C for an additional 4 h. The clear reaction mixture was cooled to 23 °C and partitioned between water (150 mL) and a 1:1 mixture of EtOAc and

hexanes (2  $\times$  150 mL). The combined organic layers were dried over  $\text{Na}_2\text{SO}_4$  and concentrated. The residue was purified by flash column chromatography ( $\text{SiO}_2$  pretreated with 5%  $\text{Et}_3\text{N}$  in hexanes, gradient elution 40%  $\rightarrow$  30% hexanes in EtOAc) to afford acetal **23** (1.85 g, 36%) as a pale yellow oil:  $R_f$  = 0.34 (50% EtOAc in hexanes,  $\text{SiO}_2$  pretreated with 5%  $\text{Et}_3\text{N}$  in hexanes); IR ( $\text{cm}^{-1}$ ) 3331;  $^1\text{H}$  NMR ( $\text{C}_6\text{D}_6$ )  $\delta$  1.71–1.77 (m, 2 H), 2.57 (t, 2 H,  $J$  = 6.8), 3.11 (s, 6 H), 3.57 (s, 2 H), 4.43 (t, 1 H,  $J$  = 5.7), 7.09–7.21 (m, 3 H), 7.27–7.30 (m, 2 H). Anal. ( $\text{C}_{12}\text{H}_{19}\text{NO}_2$ ) C, H, N.

**2-Aminopent-4-enoic Acid Methyl Ester (24).** *p*-Toluenesulfonic acid monohydrate (14.4 g, 75.7 mmol, 1.2 equiv) was added to a solution of 2-aminopent-4-enoic acid (allylglycine; 7.25 g, 62.9 mmol, 1 equiv) in  $\text{CH}_3\text{OH}$  (125 mL) at 23 °C. The reaction mixture was refluxed for 18 h and then cooled to 23 °C and concentrated. The colorless oil thus obtained was partitioned between saturated aqueous  $\text{NaHCO}_3$  (150 mL) and a 9:1 mixture of  $\text{CH}_2\text{Cl}_2$  and  $\text{CH}_3\text{OH}$  (3  $\times$  150 mL). The combined organic layers were dried over  $\text{Na}_2\text{SO}_4$  and concentrated. The residue was distilled under reduced pressure to afford 2-aminopent-4-enoic acid methyl ester (**24**) (5.00 g, 62%) as a colorless liquid: bp = 69–70 °C, 1.1 mmHg; IR ( $\text{cm}^{-1}$ ) 3379, 1740;  $^1\text{H}$  NMR ( $\text{CDCl}_3$ )  $\delta$  2.33–2.43 (m, 1 H), 2.46–2.55 (m, 1 H), 3.557 (dd, 1 H,  $J$  = 7.2, 5.1), 3.73 (s, 3 H), 5.12 (s, 1 H), 5.16–5.19 (m, 1 H), 5.68–5.80 (m, 1 H). Anal. ( $\text{C}_6\text{H}_{11}\text{NO}_2$ ) C, H, N.

**2-[3'-Benzyl-3''-(3'',3''-dimethoxypropyl)ureido]pent-4-enoic Acid Methyl Ester (25).** A solution of 2-aminopent-4-enoic acid methyl ester (**24**) (1.05 g, 8.13 mmol, 1.0 equiv) and  $\text{Et}_3\text{N}$  (1.13 mL, 8.11 mmol, 1.0 equiv) in  $\text{CH}_2\text{Cl}_2$  (10 mL) was added via cannula to a solution of triphosgene (0.803 g, 2.71 mmol, 0.33 equiv) in  $\text{CH}_2\text{Cl}_2$  (50 mL) at 23 °C. The reaction mixture was stirred for 15 min at 23 °C and then refluxed for 1.5 h. After cooling to 23 °C, a solution of **23** (1.70 g, 8.12 mmol, 1 equiv) and  $\text{Et}_3\text{N}$  (1.13 mL, 8.11 mmol, 1.0 equiv) in  $\text{CH}_2\text{Cl}_2$  (10 mL) was added via cannula. The resulting solution was stirred at 23 °C for 15 min and then partitioned between water (150 mL) and a 1:1 mixture of EtOAc and hexanes (2  $\times$  150 mL). The combined organic layers were dried over  $\text{Na}_2\text{SO}_4$  and concentrated. Purification of the residue by flash column chromatography ( $\text{SiO}_2$  pretreated with 5%  $\text{Et}_3\text{N}$  in hexanes, gradient elution 30%  $\rightarrow$  50% EtOAc in hexanes) provided urea **25** (2.61 g, 88%) as a colorless oil:  $R_f$  = 0.24 (30% EtOAc in hexanes,  $\text{SiO}_2$  pretreated with 5%  $\text{Et}_3\text{N}$  in hexanes); IR ( $\text{cm}^{-1}$ ) 3357, 1745, 1646;  $^1\text{H}$  NMR ( $\text{C}_6\text{D}_6$ )  $\delta$  1.64–1.77 (m, 2 H), 2.38–2.58 (m, 2 H), 3.07 (s, 3 H), 3.08 (s, 3 H), 3.11–3.25 (m, 2 H), 3.28 (s, 3 H), 4.30–4.48 (m, 3 H), 4.83–4.98 (m, 3 H), 5.58–5.72 (m, 2 H), 7.01–7.15 (m, 3 H), 7.21–7.24 (m, 2 H). Anal. ( $\text{C}_{19}\text{H}_{28}\text{N}_2\text{O}_5$ ) C, H, N.

**trans-2-Benzyl-6-hydroxy-1-oxooctahydropyrido[1,2-c]pyrimidine-8-carboxylic Acid Methyl Ester (26).** Trifluoroacetic acid (5 mL) was added to a solution of urea **25** (1.10 g, 3.02 mmol) in  $\text{CH}_2\text{Cl}_2$  (5 mL) at 23 °C. The reaction mixture was stirred for 2 h at 23 °C and then concentrated. The resulting yellow oil was carefully partitioned between saturated aqueous  $\text{NaHCO}_3$  (100 mL) and EtOAc (4  $\times$  100 mL). The combined organic layers were dried over  $\text{Na}_2\text{SO}_4$  and concentrated. The residue was purified by flash column chromatography (5%  $\text{CH}_3\text{OH}$  in  $\text{CH}_2\text{Cl}_2$ ) to afford alcohol **26** (0.682 g, 71%) as a white solid: mp = 144 °C;  $R_f$  = 0.14 (30% hexanes in EtOAc); IR ( $\text{cm}^{-1}$ ) 3394 (br), 1740, 1616;  $^1\text{H}$  NMR ( $\text{CDCl}_3$ )  $\delta$  1.40–1.49 (m, 1 H), 1.60 (d, 1 H,  $J$  = 2.2), 1.75–1.99 (m, 4 H), 2.51 (dq, 1 H,  $J$  = 14.6, 2.4), 3.09 (dq, 1 H,  $J$  = 11.7, 2.5), 3.36 (td, 1 H,  $J$  = 11.8, 3.8), 3.75 (s, 3 H), 3.86–3.95 (m, 1 H), 4.16–4.19 (m, 1 H), 4.55 (d, 1 H,  $J$  = 15.3), 4.66 (d, 1 H,  $J$  = 15.3), 5.27 (dd, 1 H,  $J$  = 6.8, 1.8), 7.22–7.36 (m, 5 H). Anal. ( $\text{C}_{17}\text{H}_{22}\text{N}_2\text{O}_4$ ) C, H, N.

**trans-2-Benzyl-1-oxo-6-[(*p*-tolylthio)carbonyl]oxy]octahydropyrido[1,2-c]pyrimidine-8-carboxylic Acid Methyl Ester (27).** *O*-*p*-Tolyl chlorothionoformate (1.74 mL, 11.3 mmol, 6.0 equiv) and DMAP (1.50 g, 12.3 mmol, 6.5 equiv) were added sequentially to a solution of alcohol **26** (0.600 g, 1.88 mmol, 1 equiv) in  $\text{CH}_3\text{CN}$  (25 mL) at 23 °C. The resulting cloudy suspension was refluxed for 10 h and then cooled to 23 °C and partitioned between water (100 mL) and EtOAc (4  $\times$  100 mL). The combined organic layers were dried over  $\text{Na}_2\text{SO}_4$

SO<sub>4</sub> and concentrated. Flash chromatographic purification of the residue (gradient elution 30% → 50% EtOAc in hexanes) afforded thionoformate **27** (0.444 g, 50%) as a white solid: mp = 146–149 °C;  $R_f$  = 0.53 (50% EtOAc in hexanes); IR (cm<sup>-1</sup>) 1740, 1637; <sup>1</sup>H NMR (CDCl<sub>3</sub>) δ 1.55–1.65 (m, 1 H), 1.86 (qd, 1 H,  $J$  = 11.9, 4.7), 1.95–2.06 (m, 2 H), 2.16–2.21 (m, 1 H), 2.37 (s, 3 H), 2.96–3.03 (m, 1 H), 3.10–3.16 (m, 1 H), 3.41 (td, 1 H,  $J$  = 11.9, 3.7), 3.80 (s, 3 H), 3.89–3.99 (m, 1 H), 4.54 (d, 1 H,  $J$  = 15.3), 4.72 (d, 1 H,  $J$  = 15.3), 5.40 (dd, 1 H,  $J$  = 6.8, 1.5), 5.56–5.58 (m, 1 H), 6.98 (dd, 2 H,  $J$  = 6.7, 1.7), 7.20–7.36 (m, 7 H). Anal. (C<sub>25</sub>H<sub>28</sub>N<sub>2</sub>O<sub>5</sub>S) C, H, N.

**trans-2-Benzyl-1-oxooctahydropyrido[1,2-c]pyrimidine-8-carboxylic Acid Methyl Ester (14).** Tris(trimethylsilyl)silane (0.439 mL, 1.42 mmol, 1.5 equiv) and 2,2'-azobis(2-methylpropionitrile) (AIBN; 0.031 g, 0.189 mmol, 0.20 equiv) were added sequentially to a solution of thionoformate **27** (0.444 g, 0.948 mmol, 1 equiv) in toluene (50 mL) at 23 °C. The resulting solution was deoxygenated by alternately evacuating the reaction flask and filling with argon (10 cycles) and then heated to 80 °C for 1 h. After cooling to 23 °C, the reaction mixture was partitioned between water (100 mL) and CH<sub>2</sub>Cl<sub>2</sub> (3 × 120 mL). The combined organic layers were dried over Na<sub>2</sub>SO<sub>4</sub> and concentrated. Purification of the residue by flash column chromatography (gradient elution 20% → 40% EtOAc in hexanes) provided **14** (0.260 g, 91%) as a colorless oil:  $R_f$  = 0.21 (30% EtOAc in hexanes); IR (cm<sup>-1</sup>) 1739, 1635; <sup>1</sup>H NMR (CDCl<sub>3</sub>) δ 1.19–1.30 (m, 2 H), 1.64–1.84 (m, 4 H), 1.87–1.94 (m, 1 H), 2.26–2.30 (m, 1 H), 3.07 (dq, 1 H,  $J$  = 11.6, 2.5), 3.31 (td, 1 H,  $J$  = 11.9, 4.1), 3.48–3.55 (m, 1 H), 3.75 (s, 3 H), 4.59 (s, 2 H), 5.31 (dd, 1 H,  $J$  = 6.2, 1.8), 7.22–7.35 (m, 5 H). Anal. (C<sub>17</sub>H<sub>22</sub>N<sub>2</sub>O<sub>3</sub>) C, H, N.

**trans-2-Benzyl-1-oxooctahydropyrido[1,2-c]pyrimidine-8-carboxylic Acid Benzyl Ester (15).** Sodium hydroxide (0.185 g, 4.63 mmol, 10 equiv) was added to a solution of **14** (0.140 g, 0.463 mmol, 1 equiv) in a 4:1 mixture of CH<sub>3</sub>OH and water (5 mL) at 23 °C. The resulting suspension was stirred for 4 h at 23 °C and then partitioned between aqueous HCl (1 M, 100 mL) and EtOAc (4 × 100 mL). The combined organic layers were dried over Na<sub>2</sub>SO<sub>4</sub> and concentrated to provide the corresponding carboxylic acid (0.105 g, 78% crude yield).

1-[3-(Dimethylamino)propyl]-3-ethylcarbodiimide hydrochloride (0.209 g, 1.09 mmol, 3 equiv), benzyl alcohol (0.113 mL, 1.09 mmol, 3 equiv), and DMAP (0.020 g, 0.163 mmol, 0.15 equiv) were added sequentially to a solution of the crude carboxylic acid obtained above (0.105 g, 0.364 mmol, 1 equiv) in CH<sub>2</sub>Cl<sub>2</sub> at 23 °C. The resulting suspension was stirred for 1 h at 23 °C and then partitioned between water (100 mL) and a 1:1 mixture of EtOAc and hexanes (2 × 120 mL). The combined organic layers were dried over Na<sub>2</sub>SO<sub>4</sub> and concentrated. The residue was purified by flash column chromatography (gradient elution 15% → 30% EtOAc in hexanes) to afford **15** (0.100 g, 72%) as a colorless oil:  $R_f$  = 0.30 (30% EtOAc in hexanes); IR (cm<sup>-1</sup>) 1736, 1634; <sup>1</sup>H NMR (CDCl<sub>3</sub>) δ 1.13–1.30 (m, 2 H), 1.65–1.91 (m, 5 H), 2.29–2.34 (m, 1 H), 3.06 (dq, 1 H,  $J$  = 11.6, 2.5), 3.26 (td, 1 H,  $J$  = 11.8, 4.0), 3.45–3.52 (m, 1 H), 4.52 (d, 1 H,  $J$  = 15.2), 4.65 (d, 1 H,  $J$  = 15.2), 5.16 (d, 1 H,  $J$  = 12.4), 5.22 (d, 1 H,  $J$  = 12.4), 5.36–5.38 (m, 1 H), 7.21–7.38 (m, 10 H). Anal. (C<sub>23</sub>H<sub>26</sub>N<sub>2</sub>O<sub>3</sub>) C, H, N.

**(3,3-Dimethoxypropyl)propylamine (28):** IR (cm<sup>-1</sup>) 3324; <sup>1</sup>H NMR (C<sub>6</sub>D<sub>6</sub>) δ 0.85 (t, 3 H,  $J$  = 7.4), 1.33–1.41 (m, 2 H), 1.74–1.81 (m, 2 H), 2.40 (t, 2 H,  $J$  = 7.0), 2.60 (t, 2 H,  $J$  = 6.8), 3.14 (s, 6 H), 4.49 (t, 1 H,  $J$  = 5.7). Anal. (C<sub>8</sub>H<sub>19</sub>NO<sub>2</sub>) C, H, N.

**2-[3-(3',3'-Dimethoxypropyl)-3'-propylureido]pent-4-enoic acid methyl ester (29):**  $R_f$  = 0.21 (30% EtOAc in hexanes, SiO<sub>2</sub> pretreated with 5% Et<sub>3</sub>N in hexanes); IR (cm<sup>-1</sup>) 3356, 1745, 1642; <sup>1</sup>H NMR (C<sub>6</sub>D<sub>6</sub>) δ 0.73 (t, 3 H,  $J$  = 7.4), 1.42–1.49 (m, 2 H), 1.76–1.85 (m, 2 H), 2.38–2.61 (m, 2 H), 2.96–3.22 (m, 4 H), 3.12 (s, 3 H), 3.13 (s, 3 H), 3.26 (s, 3 H), 4.39 (t, 1 H,  $J$  = 5.7), 4.84–4.90 (m, 1 H), 4.94–5.03 (m, 2 H), 5.45 (d, br, 1 H,  $J$  = 7.7), 5.66–5.77 (m, 1 H). Anal. (C<sub>15</sub>H<sub>28</sub>N<sub>2</sub>O<sub>5</sub>) C, H, N.

**trans-6-Hydroxy-1-oxo-2-propyloctahydropyrido[1,2-c]pyrimidine-8-carboxylic acid methyl ester (30):** mp = 122–123 °C;  $R_f$  = 0.09 (30% hexanes in EtOAc); IR (cm<sup>-1</sup>) 3388 (br), 1741, 1617; <sup>1</sup>H NMR (CDCl<sub>3</sub>) δ 0.90 (t, 3 H,  $J$  = 7.4), 1.37–

1.46 (m, 1 H), 1.50–1.62 (m, 2 H), 1.72–1.99 (m, 4 H), 2.47 (dq, 1 H,  $J$  = 14.3, 2.5), 3.12–3.27 (m, 2 H), 3.34–3.49 (m, 2 H), 3.71 (s, 3 H), 3.83–3.91 (m, 1 H), 4.14–4.16 (m, 1 H), 5.20 (dd, 1 H,  $J$  = 6.8, 1.7). Anal. (C<sub>13</sub>H<sub>22</sub>N<sub>2</sub>O<sub>4</sub>) C, H, N.

**trans-1-Oxo-2-propyl-6-[(p-tolylxy)thiocarbonyl]oxy]-octahydropyrido[1,2-c]pyrimidine-8-carboxylic acid methyl ester (31):** mp = 170 °C dec;  $R_f$  = 0.32 (50% EtOAc in hexanes); IR (cm<sup>-1</sup>) 1744, 1639; <sup>1</sup>H NMR (CDCl<sub>3</sub>) δ 0.91 (t, 3 H,  $J$  = 7.5), 1.52–1.66 (m, 3 H), 1.76–1.90 (m, 1 H), 1.94–2.07 (m, 2 H), 2.18 (dq, 1 H,  $J$  = 14.3, 2.8), 2.37 (s, 3 H), 2.96 (dq, 1 H,  $J$  = 15.0, 2.5), 3.15–3.28 (m, 2 H), 3.39–3.54 (m, 2 H), 3.76 (s, 3 H), 3.90 (tt, 1 H,  $J$  = 11.4, 3.2), 5.35 (dd, 1 H,  $J$  = 6.9, 1.9), 5.53–5.57 (m, 1 H), 6.98 (d, 2 H,  $J$  = 8.4), 7.21 (d, 2 H,  $J$  = 8.4). Anal. (C<sub>21</sub>H<sub>28</sub>N<sub>2</sub>O<sub>5</sub>S) C, H, N.

**trans-1-Oxo-2-propyloctahydropyrido[1,2-c]pyrimidine-8-carboxylic acid methyl ester (16):**  $R_f$  = 0.16 (30% EtOAc in hexanes); IR (cm<sup>-1</sup>) 1741, 1635; <sup>1</sup>H NMR (CDCl<sub>3</sub>) δ 0.89 (t, 1 H,  $J$  = 7.3), 1.12–1.32 (m, 2 H), 1.49–1.84 (m, 6 H), 1.95 (dq, 1 H,  $J$  = 13.1, 3.4), 2.21–2.27 (m, 1 H), 3.13 (ddd, 1 H,  $J$  = 11.5, 5.0, 2.8), 3.19–3.52 (m, 4 H), 3.71 (s, 3 H), 5.24 (dd, 1 H,  $J$  = 6.2, 1.9). Anal. (C<sub>13</sub>H<sub>22</sub>N<sub>2</sub>O<sub>3</sub>) C, H, N.

**trans-1-Oxo-2-propyloctahydropyrido[1,2-c]pyrimidine-8-carboxylic acid benzyl ester (17):**  $R_f$  = 0.24 (30% EtOAc in hexanes); IR (cm<sup>-1</sup>) 1737, 1636; <sup>1</sup>H NMR (CDCl<sub>3</sub>) δ 0.87 (t, 3 H,  $J$  = 7.5), 1.15–1.25 (m, 2 H), 1.45–1.81 (m, 6 H), 1.90 (dq, 1 H,  $J$  = 13.1, 3.2), 2.25–2.31 (m, 1 H), 3.10 (ddd, 1 H,  $J$  = 11.7, 4.9, 2.5), 3.17–3.41 (m, 4 H), 5.11 (d, 1 H,  $J$  = 12.5), 5.19 (d, 1 H,  $J$  = 12.5), 5.32 (dd, 1 H,  $J$  = 6.4, 2.0), 7.30–7.36 (m, 5 H). Anal. (C<sub>19</sub>H<sub>26</sub>N<sub>2</sub>O<sub>3</sub>) C, H, N.

**Acknowledgment.** We are grateful for many helpful discussions throughout the course of this work with Prof. Henry Rappoport, Drs. Robert Babine, Wesley Chong, Thomas Hendrickson, Susumu Katoh, Hiroshi Kawakami, Nobuyuki Okajima, Anna Tempczyk, and Leora Zalman, Mr. Hiroki Tada, Ms. Angelica Linton, and Mr. Ted Bleckman. We also thank Dr. Raj K. Chadha of The Scripps Research Institute for obtaining the X-ray crystal structure of compound **26**.

**Supporting Information Available:** ORTEP diagram of compound **26** with relevant crystal structure data (7 pages). Ordering information is given on any current masthead page.

## References

- (1) Tanaka, H.; Kuroda, A.; Marusawa, H.; Hatanaka, H.; Kino, T.; Goto, T.; Hashimoto, M.; Taga, T. Structure of FK506: A Novel Immunosuppressant Isolated from *Streptomyces*. *J. Am. Chem. Soc.* **1987**, *109*, 5031–5033.
- (2) For recent reviews on this class of immunosuppressants, see: (a) Schreiber, S. L.; Albers, M. W.; Brown, E. J. The Cell Cycle, Signal Transduction, and Immunophilin-Ligand Complexes. *Acc. Chem. Res.* **1993**, *26*, 412–420. (b) Armistead, D. M.; Harding, M. W. Immunophilins and Immunosuppressive Drug Action. *Annu. Rep. Med. Chem.* **1993**, *28*, 207–215. (c) Belshaw, P. J.; Meyer, S. D.; Johnson, D. D.; Romo, D.; Ikeda, Y.; Andrus, M.; Alberg, D. G.; Schultz, L. W.; Clardy, J.; Schreiber, S. L. Synthesis, Structure and Mechanism in Immunophilin Research. *Synlett* **1994**, 381–392. (d) Wiederrecht, G.; Etzkorn, F. The Immunophilins. *Perspect. Drug Discovery Des.* **1994**, *2*, 57–84. (e) O'Keefe, S. J.; O'Neill, E. A. Cyclosporin A and FK506: Immunosuppression, Inhibition of Transcription and the Role of Calcineurin. *Perspect. Drug Discovery Des.* **1994**, *2*, 85–102.
- (3) (a) Siekierka, J. J.; Hung, S. H. Y.; Poe, M.; Lin, C. S.; Sigal, N. H. A Cytosolic-Binding Protein for the Immunosuppressant FK506 has Isomerase Activity but is Distinct from Cyclophilin. *Nature* **1989**, *341*, 755–757. (b) Harding, M. W.; Galat, A.; Uehling, D. E.; Schreiber, S. L. A Receptor for the Immunosuppressant FK506 is a Cis-Trans Peptidyl-Prolyl Isomerase. *Nature* **1989**, *341*, 758–760. (c) Siekierka, J. J.; Wiederrecht, G.; Greulich, H.; Boulton, D.; Hung, S. H. Y.; Cryan, J.; Hodges, P. J.; Sigal, N. H. The Cytosolic-Binding Protein for the Immunosuppressant FK506 is Both a Ubiquitous and Highly Conserved Peptidyl-Prolyl Cis-Trans Isomerase. *J. Biol. Chem.* **1990**, *265*, 21011–21015.
- (4) Additional members of a group of proteins which bind FK506 have been identified and collectively named FKBP. The 12 kDa protein originally termed FKBP is currently referred to as FKBP12. For the characterization of other (higher molecular weight) members of this family of proteins, see: Baughman, G.;

- Wiederrecht, G. J.; Campbell, N. F.; Martin, M. M.; Bourgeois, S. FKBP51, a Novel T-Cell Specific Immunophilin Capable of Calcineurin Inhibition. *Mol. Cell. Biol.* **1995**, *15*, 4395–4402 and references therein. See also: Fischer, G. Peptidyl-Prolyl *cis/trans* Isomerases and Their Effectors. *Angew. Chem., Int. Ed. Engl.* **1994**, *33*, 1415–1436.
- (5) (a) Rosen, M. K.; Standaert, R. F.; Galat, A.; Nakatsuka, M.; Schreiber, S. L. Inhibition of FKBP Rotamase Activity by Immunosuppressant FK506: Twisted Amide Surrogate. *Science* **1990**, *248*, 863–866. (b) Albers, M. W.; Walsh, C. T.; Schreiber, S. L. Substrate Specificity for the Human Rotamase FKBP: A View of FK506 and Rapamycin as Leucine-(Twisted Amide)-Proline Mimics. *J. Org. Chem.* **1990**, *55*, 4984–4986.
  - (6) Rügger, A.; Kuhn, M.; Lichti, H.; Loosli, H.-R.; Huguenin, R.; Quiquerez, C.; von Wartburg, A. Cyclosporin A, a Peptide Metabolite from *Trichoderma polysporum* (LINK ex PERS.) *Rifai*, with a Remarkable Immunosuppressive Activity. *Helv. Chim. Acta* **1976**, *59*, 1075–1092.
  - (7) (a) Takahashi, N.; Hayano, T.; Suzuki, M. Peptidyl-Prolyl *cis-trans* Isomerase is the Cyclosporin A-Binding Protein Cyclophilin. *Nature* **1989**, *337*, 473–475. (b) Fischer, G.; Wittman-Liebold, B.; Lang, K.; Kiefhaber, T.; Schmid, F. X. Cyclophilin and Peptidyl-Prolyl *cis-trans* Isomerase are Probably Identical Proteins. *Nature* **1989**, *337*, 476–478.
  - (8) Findlay, J. A.; Radics, L. On the Chemistry and High Field Nuclear Magnetic Resonance Spectroscopy of Rapamycin. *Can. J. Chem.* **1980**, *58*, 579–590.
  - (9) (a) Bierer, B. E.; Mattila, P. S.; Standaert, R. F.; Herzenberg, L. A.; Burakoff, S. J.; Crabtree, G.; Schreiber, S. L. Two Distinct Signal Transmission Pathways in T Lymphocytes are Inhibited by Complexes Formed Between an Immunophilin and Either FK506 or Rapamycin. *Proc. Natl. Acad. Sci. U.S.A.* **1990**, *87*, 9231–9235. (b) Dumont, F. J.; Melino, M. R.; Staruch, M. J.; Koprak, S. L.; Fischer, P. A.; Sigal, N. H. The Immunosuppressive Macrolides FK506 and Rapamycin act as Reciprocal Antagonists in Murine T-cells. *J. Immunol.* **1990**, *144*, 1418–1424.
  - (10) (a) Klee, C. B.; Draetta, G. F.; Hubbard, M. J. Calcineurin. *Adv. Enzymol. Relat. Areas Mol. Biol.* **1988**, *61*, 149–200. (b) Pallan, C.; Sharma, R. K.; Wang, J. H. Regulation of Calcineurin: A Multifunctional Calmodulin-Stimulated Phosphatase. In *Calcium Binding Proteins, Characterization and Properties, Vol. 1*; Thompson, M. P., Ed.; CRC Press: Boca Raton, FL, 1988; pp 51–82.
  - (11) (a) Liu, J.; Farmer, J. D., Jr.; Lane, W. S.; Friedman, J.; Weissman, I.; Schreiber, S. L. Calcineurin is a Common Target of Cyclophilin-Cyclosporin A and FKBP-FK506 Complexes. *Cell* **1991**, *66*, 807–815. (b) Fruman, D. A.; Klee, C. B.; Bierer, B. E.; Burakoff, S. J. Calcineurin Phosphatase Activity in T Lymphocytes is Inhibited by FK506 and Cyclosporin A. *Proc. Natl. Acad. Sci. U.S.A.* **1992**, *89*, 3686–3690.
  - (12) (a) Flanagan, W. M.; Corthésy, B.; Bram, R. J.; Crabtree, G. R. Nuclear Association of a T-Cell Transcription Factor Blocked by FK506 and Cyclosporin A. *Nature* **1991**, *352*, 803–807. (b) Dumont, F. J.; Staruch, M. J.; Koprak, S. L.; Melino, M. R.; Sigal, N. H. Distinct Mechanisms of Suppression of Murine T-Cell Activation by the Related Macrolides FK506 and Rapamycin. *J. Immunol.* **1990**, *144*, 251–258. (c) Tocci, M. J.; Matkovich, D. A.; Collier, K. A.; Kwok, P.; Dumont, F.; Lin, S.; Degudicibus, S.; Siekierka, J. J.; Chin, J.; Hutchinson, N. I. The Immunosuppressant FK506 Selectively Inhibits Expression of Early T-Cell Activation Genes. *J. Immunol.* **1989**, *143*, 718–726.
  - (13) Bierer, B. E.; Somers, P. K.; Wandless, T. J.; Burakoff, S. J.; Schreiber, S. L. Probing Immunosuppressant Action with a Nonnatural Immunophilin Ligand. *Science* **1990**, *250*, 556–559.
  - (14) Lepre, C. A.; Pearlman, D. A.; Cheng, J.-W.; DeCenzo, M. T.; Livingston, D. J.; Moore, J. M. Solution Structure of FK506 Bound to the R42K, H87V Double Mutant of FKBP-12. *Biochemistry* **1994**, *33*, 13571–13580. See also: Meadows, R. P.; Nettesheim, D. G.; Xu, R. X.; Olejniczak, E. T.; Petros, A. M.; Holzman, T. F.; Severin, J.; Gubbins, E.; Smith, H.; Fesik, S. W. Three-Dimensional Structure of the FK506 Binding Protein/Ascomycin Complex in Solution by Heteronuclear Three- and Four-Dimensional NMR. *Biochemistry* **1993**, *32*, 754–765.
  - (15) (a) Van Duyne, G. D.; Standaert, R. F.; Karplus, P. A.; Schreiber, S. L.; Clardy, J. Atomic Structure of FKBP-FK506, an Immunophilin-Immunosuppressant Complex. *Science* **1991**, *252*, 839–842. (b) Van Duyne, G. D.; Standaert, R. F.; Karplus, P. A.; Schreiber, S. L.; Clardy, J. Atomic Structures of the Human Immunophilin FKBP-12 Complexes with FK506 and Rapamycin. *J. Mol. Biol.* **1993**, *229*, 105–124. (c) Clardy, J. Structural Studies on FK506, Cyclosporin A and Their Immunophilin Complexes. *Perspect. Drug Discovery Des.* **1994**, *2*, 127–144. (d) Wilson, K. P.; Yamashita, M. M.; Sintchak, M. D.; Rotstein, S. H.; Murcko, M. A.; Boger, J.; Thomson, J. A.; Fitzgibbon, M. J.; Black, J. R.; Navia, M. A. Comparative X-ray Structures of the Major Binding Protein for the Immunosuppressant FK506 (Tacrolimus) in Unligated Form and in Complex with FK506 and Rapamycin. *Acta Crystallogr.* **1995**, *D51*, 511–521.
  - (16) (a) Griffith, J. P.; Kim, J. L.; Kim, E. E.; Sintchak, M. D.; Thomson, J. A.; Fitzgibbon, M. J.; Fleming, M. A.; Caron, P. R.; Hsiao, K.; Navia, M. A. X-ray Structure of Calcineurin Inhibited by the Immunophilin-Immunosuppressant FKBP12-FK506 Complex. *Cell* **1995**, *82*, 507–522. (b) Kissinger, C. R.; Parge, H. E.; Knighton, D. R.; Lewis, C. T.; Pelletier, L. A.; Tempczyk, A.; Kalish, V. J.; Tucker, K. D.; Showalter, R. E.; Moomaw, E. W.; Gastinel, L. N.; Habuka, N.; Chen, X.; Maldonado, F.; Barker, J. E.; Bacquet, R.; Villafranca, J. E. Crystal Structures of Human Calcineurin and the Human FKBP12-FK506-Calcineurin Complex. *Nature* **1995**, *378*, 641–644.
  - (17) For a discussion of the possible intricacies of calcineurin inhibition by the FKBP12–FK506 complex, see refs 15d and 16a.
  - (18) For an excellent review of FK506 structure–activity studies, see: Goulet, M. T.; Rupprecht, K. M.; Sinclair, P. J.; Wyvratt, M. J.; Parsons, W. H. The Medicinal Chemistry of FK506. *Perspect. Drug Discovery Des.* **1994**, *2*, 145–162.
  - (19) (a) Aldape, R. A.; Futer, O.; DeCenzo, M. T.; Jarrett, B. P.; Murcko, M. A.; Livingston, D. J. Charged Surface Residues of FKBP12 Participate in Formation of the FKBP12-FK506-Calcineurin Complex. *J. Biol. Chem.* **1992**, *267*, 16029–16032. (b) Yang, D.; Rosen, M. K.; Schreiber, S. L. A Composite FKBP12-FK506 Surface That Contacts Calcineurin. *J. Am. Chem. Soc.* **1993**, *115*, 819–820. (c) Futer, O.; DeCenzo, M. T.; Aldape, R. A.; Livingston, D. J. FK506 Binding Protein Mutational Analysis. *J. Biol. Chem.* **1995**, *270*, 18935–18940.
  - (20) (a) Armistead, D. A.; Boger, J. S.; Meyers, H. V.; Saunders, J. O.; Tung, R. D. Immunosuppressive Compounds. U.S. Patent 5 192 773, 1993. (b) Holt, D. A.; Luengo, J. I.; Yamashita, D. S.; Oh, H.-J.; Konialian, A. L.; Yen, H.-K.; Rozamus, L. W.; Brandt, M.; Bossard, M. J.; Levy, M. A.; Eggleston, D. S.; Liang, J.; Schultz, L. W.; Stout, T. J.; Clardy, J. Design, Synthesis, and Kinetic Evaluation of High-Affinity FKBP Ligands and the X-ray Crystal Structures of Their Complexes with FKBP12. *J. Am. Chem. Soc.* **1993**, *115*, 9925–9938. (c) Holt, D. A.; Konialian-Beck, A. L.; Oh, H.-J.; Yen, H.-K.; Rozamus, L. W.; Krog, A. J.; Erhard, K. F.; Ortiz, E.; Levy, M. A.; Brandt, M.; Bossard, M. J.; Luengo, J. I. Structure-Activity Studies of Synthetic FKBP Ligands as Peptidyl-Prolyl Isomerase Inhibitors. *Bioorg. Med. Chem. Lett.* **1994**, *4*, 315–320. (d) Luengo, J. I.; Konialian-Beck, A.; Levy, M. A.; Brandt, M.; Eggleston, D. S.; Holt, D. A. Synthesis and Structure-Activity Relationships of Macrocyclic FKBP Ligands. *Bioorg. Med. Chem. Lett.* **1994**, *4*, 321–324. (e) Yamashita, D. S.; Oh, H.-J.; Yen, H.-K.; Bossard, M. J.; Brandt, M.; Levy, M. A.; Newman-Tarr, T.; Badger, A.; Luengo, J. I.; Holt, D. A. Design, Synthesis and Evaluation of Dual Domain FKBP Ligands. *Bioorg. Med. Chem. Lett.* **1994**, *4*, 325–328. (f) Wang, G. T.; Lane, B.; Fesik, S. W.; Petros, A.; Luly, J.; Krafft, G. A. Synthesis and FKBP Binding of Small Molecule Mimics of the Tricarbonyl Region of FK506. *Bioorg. Med. Chem. Lett.* **1994**, *4*, 1161–1166. (g) Birkenshaw, T. N.; Caffrey, M. V.; Cladingboel, D. E.; Cooper, M. E.; Donald, D. K.; Furber, M.; Hardern, D. N.; Harrison, R. P.; Marriott, D. P.; Perry, M. W. D.; Stocks, M. J.; Teague, S. J.; Withnall, W. J. Synthetic FKBP12 Ligands. Design and Synthesis of Pyranose Replacements. *Bioorg. Med. Chem. Lett.* **1994**, *4*, 2501–2506. (h) Caffrey, M. V.; Cladingboel, D. E.; Cooper, M. E.; Donald, D. K.; Furber, M.; Hardern, D. N.; Harrison, R. P.; Stocks, M. J.; Teague, S. J. Synthesis and Evaluation of Dual Domain Macrocyclic FKBP12 Ligands. *Bioorg. Med. Chem. Lett.* **1994**, *4*, 2507–2510. (i) Armistead, D. M.; Badia, M. C.; Deininger, D. D.; Duffy, J. P.; Saunders, J. O.; Tung, R. D.; Thomson, J. A.; DeCenzo, M. T.; Futer, O.; Livingston, D. J.; Murcko, M. A.; Yamashita, M. M.; Navia, M. A. Design, Synthesis and Structure of Non-macrocyclic Inhibitors of FKBP12, the Major Binding Protein for the Immunosuppressant FK506. *Acta Crystallogr.* **1995**, *D51*, 522–528. (j) Tatlock, J. H.; Kalish, V. J.; Parge, H. E.; Knighton, D. R.; Showalter, R. E.; Lewis, C. T.; French, J. V.; Villafranca, J. E. High-Affinity FKBP-12 Ligands Derived from (R)-(-)-Carvone. Synthesis and Evaluation of FK506 Pyranose Ring Replacements. *Bioorg. Med. Chem. Lett.* **1995**, *5*, 2489–2494.
  - (21) (a) Hauske, J. R.; Dorff, P.; Julin, S.; DiBrino, J.; Spencer, R.; Williams, R. Design and Synthesis of Novel FKBP Inhibitors. *J. Med. Chem.* **1992**, *35*, 4284–4296. (b) Andres, C. J.; MacDonald, T. L.; Ocain, T. D.; Longhi, D. Conformationally Defined Analogs of Prolylamides. *trans-Prolyl Peptidomimetics*. *J. Org. Chem.* **1993**, *58*, 6609–6613. (c) Babine, R. E.; Bleckman, T. M.; Kissinger, C. R.; Showalter, R.; Pelletier, L. A.; Lewis, C.; Tucker, K.; Moomaw, E.; Parge, H. E.; Villafranca, J. E. Design, Synthesis and X-ray Crystallographic Studies of Novel FKBP-12 Ligands. *Bioorg. Med. Chem. Lett.* **1995**, *5*, 1719–1724. (d) Reference 20c.
  - (22) (a) Duffy, J. P. Novel Immunosuppressive Compounds. International Patent Application WO 92/21313, 1992. (b) Reference 20c.
  - (23) A non-macrocyclic molecule which associates with FKBP12 at the 0.20  $\mu$ M level and displays calcineurin inhibitory properties has been reported; see: Andrus, M. B.; Schreiber, S. L. Structure-

- Based Design of an Acyclic Ligand That Bridges FKBP12 and Calcineurin. *J. Am. Chem. Soc.* **1993**, *115*, 10420–10421. See also: Furber, M. FKBP12-Ligand-Calcineurin Interactions: Analogues of SBL506. *J. Am. Chem. Soc.* **1995**, *117*, 7267–7268.
- (24) Greer, J.; Erickson, J. W.; Baldwin, J. J.; Varney, M. D. Application of the Three-Dimensional Structures of Protein Target Molecules in Structure-Based Drug Design. *J. Med. Chem.* **1994**, *37*, 1035–1054 and references therein.
- (25) Michnick, S. W.; Rosen, M. K.; Wandless, T. J.; Karplus, M.; Schreiber, S. L. Solution Structure of FKBP, a Rotamase Enzyme and Receptor for FK506 and Rapamycin. *Science* **1991**, *252*, 836–839.
- (26) The observed locations in the FKBP12–FK506 complex of the FKBP12 residues determined to interact with calcineurin are assumed to be desirable. However, slight movement of these residues from the above positions has been noted in the crystal structure of the calcineurin–FKBP12–FK506 ternary complex.<sup>16a</sup>
- (27) (a) Wiley, R. A.; Rich, D. H. Peptidomimetics Derived From Natural Products. *Med. Res. Rev.* **1993**, *13*, 368–378. (b) Petros, A. M.; Luly, J. R.; Liang, H.; Fesik, S. W. Conformation of an FK506 Analog in Aqueous Solution is Similar to the FKBP-Bound Conformation of FK506. *J. Am. Chem. Soc.* **1993**, *115*, 9920–9924.
- (28) Majer, P.; Randad, R. S. A Safe and Efficient Method for Preparation of *N,N*-Unsymmetrically Disubstituted Ureas Utilizing Triphosgene. *J. Org. Chem.* **1994**, *59*, 1937–1938.
- (29) Kotani, R. Demjanov Rearrangement of 1-Methylcyclohexyl-methylamine. *J. Org. Chem.* **1965**, *30*, 350–354.
- (30) Johnson, R. L.; Rajakumar, G.; Yu, K.-L.; Mishra, R. K. Synthesis of Pro-Leu-Gly-NH<sub>2</sub> Analogues Modified at the Prolyl Residue and Evaluation of Their Effects on the Receptor Binding Activity of the Central Dopamine Receptor Agonist, ADTN. *J. Med. Chem.* **1986**, *29*, 2104–2107.
- (31) Brown, H. C.; Krishnamurthy, S.; Stocky, T. P. Selective Reductions. XIX. The Rapid Reaction of Carboxylic Acids with Borane-Tetrahydrofuran. A Remarkably Convenient Procedure for the Selective Conversion of Carboxylic Acids to the Corresponding Alcohols in the Presence of Other Functional Groups. *J. Org. Chem.* **1973**, *38*, 2786–2792.
- (32) The identity of the major acyclic urea isomer (cis or trans) in chloroform solution is currently unknown.
- (33) For use of related *N*-acyliminium ion cyclization reactions in alkaloid synthesis, see: (a) Hart, D. J. Effect of A<sup>(1,3)</sup> Strain on the Stereochemical Course of *N*-Acyliminium Ion Cyclizations. *J. Am. Chem. Soc.* **1980**, *102*, 397–398. (b) Hart, D. J.; Kanai, K.-i. New Approach to Lythraceae Alkaloids: Total Synthesis of (±)-Vertaline. *J. Org. Chem.* **1982**, *47*, 1555–1560. (c) Hart, D. J.; Yang, T.-K. *N*-Acyliminium Ion Rearrangements: Generalities and Application to the Synthesis of Pyrrolizidine Alkaloids. *J. Org. Chem.* **1985**, *50*, 235–242.
- (34) Review: Speckamp, W. N.; Hiemstra, H. Intramolecular Reactions of *N*-Acyliminium Intermediates. *Tetrahedron* **1985**, *41*, 4367–4416.
- (35) The formation of diastereomeric alcohol and olefinic products in related *N*-acyliminium ion cyclization reactions has been reported. See refs 33b,c.
- (36) Robins, M. J.; Wilson, J. S.; Hansske, F. Nucleic Acid Related Compounds. 42. A General Procedure for the Efficient Deoxygenation of Secondary Alcohols. Regiospecific and Stereoselective Conversion of Ribonucleosides to 2'-Deoxynucleosides. *J. Am. Chem. Soc.* **1983**, *105*, 4059–4065.
- (37) Schummer, D.; Höfle, G. Tris(trimethylsilyl)silane as a Reagent for the Radical Deoxygenation of Alcohols. *Synlett* **1990**, 705–706.
- (38) Still, W. C.; Kahn, M.; Mitra, A. Rapid Chromatographic Technique for Preparative Separations with Moderate Resolution. *J. Org. Chem.* **1978**, *43*, 2923–2925.
- (39) Standaert, R. F.; Galat, A.; Verdine, G. L.; Schreiber, S. L. Molecular Cloning and Overexpression of the Human FK506-Binding Protein FKBP. *Nature* **1990**, *346*, 671–674.
- (40) X-PLOR, version 3.1. Brünger, A. T. *X-PLOR v3.1 Manual*; Yale University Press: New Haven, CT, 1992.
- (41) Quanta, version 4.1, is produced by BIOSYM/Molecular Simulations, Inc., 16 New England Executive Park, Burlington, MA 01803-5297.
- (42) McRee, D. E. A Visual Protein Crystallographic Software System for X11/Xview. *J. Mol. Graph.* **1992**, *10*, 44–47.
- (43) Kofron, J. L.; Kuzmic, P.; Kishore, V.; Colón-Bonilla, E.; Rich, D. H. Determination of Kinetic Constants for Peptidyl Prolyl cis-trans Isomerases by an Improved Spectrophotometric Assay. *Biochemistry* **1991**, *30*, 6127–6134.
- (44) (a) Harrison, R. K.; Stein, R. L. Substrate Specificities of the Peptidyl Prolyl cis-trans Isomerase Activities of Cyclophilin and FK-506 Binding Protein: Evidence for the Existence of a Family of Distinct Enzymes. *Biochemistry* **1990**, *29*, 3813–3816. (b) Reference 9a.

JM950798A